

1 Improving Differential-Neural Cryptanalysis with 2 Inception

3 Liu Zhang^{1,2}, Zilong Wang^{1,2}, and Baocang Wang³

4 ¹ School of Cyber Engineering, Xidian University, Xi'an, China,
5 liuzhang@stu.xidian.edu.cn, zlwang@xidian.edu.cn

6 ² State Key Laboratory of Cryptology, P.O.Box 5159, Beijing 100878, China

7 ³ State Key Laboratory of Integrated Service Networks, Xidian University, Xi'an,
8 China, bcwang79@aliyun.com

9 **Abstract.** In CRYPTO'19, Gohr proposed a new cryptanalysis method
10 by building the differential-neural distinguisher with a neural network.
11 Gohr combined a differential-neural distinguisher with a classical differ-
12 ential, achieving a 12-round (out of 22) key recovery attack on SPECK32/
13 64. Bao *et al.* improved the classical differential by generalizing the
14 concept of neutral bits, leading to key recovery attacks for 13-round
15 SPECK32/64 and 16-round (out of 32) SIMON32/64.

16 Our primary objective is to enhance the differential-neural distinguisher's
17 capabilities by applying deep learning techniques, focusing on handling
18 more rounds and improving accuracy. We adopt a design inspired by the
19 Inception Block in GoogLeNet to effectively capture information across
20 multiple dimensions, employing multiple parallel convolutional layers
21 with different kernel sizes positioned before the Residual Network. In the
22 case of SPECK32/64, our efforts yield accuracy improvements in rounds 6,
23 7, and 8, enabling the successful training of a 9-round differential-neural
24 distinguisher. As for SIMON32/64, we develop a differential-neural distin-
25 guisher capable of effectively handling 12 rounds while achieving note-
26 worthy accuracy enhancements in rounds 9, 10, and 11. Additionally, we
27 utilize neutral bits to ensure the required data distribution for launching
28 a successful key recovery attack using multiple-ciphertext pairs as input
29 for the neural network.

30 Combining these various advancements allows us to considerably re-
31 duce the time and data complexity of key recovery attacks on 13-round
32 SPECK32/64. In particular, we achieve a successful 14-round key recovery
33 attack by exhaustively guessing a 1-round subkey, marking a significant
34 milestone in differential-neural cryptanalysis. In the case of SIMON32/64,
35 we accomplish a groundbreaking 17-round key recovery attack for the
36 first time and reduce the time complexity of the 16-round key recovery
37 attack.

38 **Keywords:** Differential-Neural Distinguisher · Inception · SPECK · SI-
39 MON · Key Recovery Attack

40 1 Introduction

41 In CRYPTO 2019, Gohr [12] proposed the idea of differential-neural cryptanaly-
 42 sis. The differential-neural distinguisher, trained by the neural network, is intro-
 43 duced as the underlying distinguisher. Bayesian search speeds up key recovery
 44 attacks compared to classical differential cryptanalysis. The differential-neural
 45 distinguisher can distinguish whether ciphertexts are encrypted by plaintexts
 46 that satisfy a specific input difference or by random numbers. However, the cur-
 47 rent differential-neural distinguisher seems only effective for limited rounds of
 48 ciphertext. Therefore, a short high-probability classical differential $\Delta S \rightarrow \Delta P$
 49 is prepended before the differential-neural distinguisher to increase the number
 50 of rounds for key recovery attacks.

51 Gohr [12] showed that the Residual Network [14] could capture the non-
 52 randomness of the distribution of output pairs when the input pairs of round-
 53 reduced SPECK32/64 meet a specific difference. As a result, 6, 7, and 8-round
 54 differential-neural distinguishers were trained, and 11, 12-round key recovery
 55 attacks for SPECK32/64 were achieved by combining a 2-round classical differ-
 56 ential. There may be two directions to improve differential-neural cryptanalysis.
 57 One is to use a longer classical differential prepended on top of the differential-
 58 neural distinguisher. Bao *et al.* [3] generalized the concept of neutral bits and
 59 searched for (conditional) simultaneous neutral bit-set with a higher probabili-
 60 ty for more rounds of the classical differential. Thus, Bao *et al.* devised a new
 61 13-round key recovery attack for SPECK32/64 with the same differential-neural
 62 distinguisher proposed in [12]. The other is to study the effective differential-
 63 neural distinguisher with more rounds. Chen *et al.* [9] and Benamira [5] *et al.*
 64 almost simultaneously proposed the method of using multiple-ciphertext pairs
 65 instead of single-ciphertext pairs (in Gohr’s work) as input of the neural network,
 66 both improved the accuracy of the 6, 7-round differential-neural distinguisher of
 67 SPECK32/64. Bao *et al.* [3] used the Dense Network [16] and the Squeeze-and-
 68 Excitation Network [15] to train differential-neural distinguisher, obtained 9, 10,
 69 and 11-round differential-neural distinguisher and devised a 16-round key recov-
 70 ery attack for SIMON32/64. To obtain more information from the ciphertext, we
 71 made some improvements for differential-neural cryptanalysis, as listed below.

72 **Our contribution.** The contributions of this work include the following:

- 73 - We have developed an enhanced differential-neural distinguisher by modifying
 74 the network architecture. To achieve this, we have introduced an Inception
 75 module composed of multiple-parallel convolutional layers before the Residual
 76 Network. Incorporating the Inception module is to capture a broader range
 77 of information across various dimensions within the ciphertext pairs. We have
 78 also made some adjustments to the convolutional kernel size according to the
 79 round functions of the cipher. As a result of these improvements, we have
 80 observed enhanced accuracy in the 6, 7, and 8-round differential-neural distin-
 81 guishers, and we have trained a new 9-round differential-neural distinguisher
 82 for SPECK32/64. Similarly, we have improved the accuracy of the 9, 10, and 11-

83 round distinguishers and developed a new 12-round differential-neural distin-
 84 guisher for SIMON32/64. Tables 2 and 5 present the results of the differential-
 85 neural distinguisher for SPECK32/64 and SIMON32/64, respectively.

86 - To execute a key recovery attack successfully, each ciphertext pair in multiple-
 87 ciphertext pairs acquired through classical differentials must exhibit the same
 88 difference. Taking inspiration from Gohr’s work on the combined response of
 89 the differential-neural distinguisher, we leverage neutral bits with a probabilit-
 90 ity of one to generate multiple-plaintext pairs. Subsequently, we encrypt these
 91 multiple-plaintext pairs, resulting in the generation of multiple-ciphertext pairs.
 92

93 - We successfully implemented several key recovery attacks using the improved
 94 differential-neural distinguisher with a classical differential. We reduce the time
 95 and data complexity of the key recovery attack for the 13-round SPECK32/64.
 96 In particular, we successfully implemented a 14-round key recovery attack
 97 by exhaustively guessing a 1-round subkey, marking the first instance of a 14-
 98 round key recovery attack in differential-neural cryptanalysis. For SIMON32/64,
 99 we can implement a 17-round key recovery attack using deep learning methods
 100 for the first time. In addition, we reduce the time complexity of the 16-round
 101 key recovery attack. Detailed experimental comparisons are shown in Table 1.
 102 Source codes are available in [https://github.com/CryptAnalystDesigner/
 103 NeuralDistinguisherWithInception.git](https://github.com/CryptAnalystDesigner/NeuralDistinguisherWithInception.git).

104 **Organization.** Section 2 gives the preliminary on the distinguisher model, the
 105 key recovery attack process, and generalized neutral bits. Section 3 introduces the
 106 training method and the result for SPECK32/64. We introduce data generation,
 107 experimental environment, and complexity calculation in Section 4. Section 5
 108 presents the details of our 13, 14-round key recovery attacks for SPECK32/64.
 109 Section 6 introduces the training method and the result for SIMON32/64. Section
 110 7 exhibits the details of our 16, 17-round key recovery attacks for SIMON32/64.
 111 We conclude the paper in Section 8.

112 2 Preliminary

113 2.1 Brief Description of SPECK32/64 and SIMON32/64

114 Let ω be the word size (the number of bits of a word), and the block size can be
 115 denoted as L bits, where $L = 2\omega$. Let (x_r, y_r) be the left and right branches of a
 116 state after encryption of r rounds, k_i the subkey of i rounds. Denote the bitwise
 117 XOR by \oplus , the addition modulo 2^ω by \boxplus , the bitwise AND by \cdot , the bitwise
 118 right rotation by \ggg , and the bitwise left rotation by \lll .

SPECK32/64 and SIMON32/64 are members in the lightweight block cipher family SPECK and SIMON [4]. The round function (out of 22) of SPECK32/64 takes a 16-bit subkey k_i and a state consisting of two 16-bit words (x_i, y_i) as

Table 1. Summary of key recovery attacks on SPECK32/64 and SIMON32/64

Target	r	Dist.	Conf.	Time	Data	Succ. Rate	Key Space	Ref.
SPECK 32/64		\mathcal{DD}	1+8+4	2^{57}	2^{25}	–	2^{64}	[10]
		\mathcal{DD}	1+8+2+2	$2^{50.16}$	$2^{31.13}$	63%	2^{64}	[8]
	13	\mathcal{DD}	2+8+3	$2^{55.58}$	$2^{24.26}$	–	2^{64}	[11]
		\mathcal{ND}	1+3+8+1	$2^{48.67+2.4^*}$	2^{29}	82%	2^{63}	[3]
		\mathcal{ND}	1+3+8+1	$2^{46.05+2.92}/2^{41.44+2.92^\dagger}$	2^{27}	21%	2^{63}	Sect.5.2
		\mathcal{DD}	1+9+4	$2^{62.47}$	$2^{30.47}$	–	2^{64}	[18]
		\mathcal{DD}	1+9+2+2	$2^{60.99}$	$2^{31.75}$	63%	2^{64}	[8]
	14	\mathcal{DD}	2+9+3	$2^{60.58}$	$2^{30.26}$	76%	2^{64}	[11]
		\mathcal{ND}	1+3+8+1+1	$2^{62.05+2.92}/2^{57.44+2.92^\dagger}$	2^{27}	21%	2^{63}	Sect.5.3
		\mathcal{DD}	2+12+2	$2^{26.48}$	$2^{29.48}$	62%	2^{64}	[2]
SIMON 32/64	16	\mathcal{ND}	1+3+11+1	$2^{41.81+2.4^*}$	2^{21}	49%	2^{64}	[3]
		\mathcal{ND}	1+3+11+1	$2^{40.12+2.92}/2^{33.60+2.92^\dagger}$	2^{22}	80%	2^{64}	Sect.7.1
	17	\mathcal{ND}	1+4+11+1	$2^{47.25+2.92}/2^{40.64+2.92^\dagger}$	2^{28}	9%	2^{64}	Sect.7.2
	18	\mathcal{DD}	1+13+4	$2^{46.00}$	$2^{31.2}$	63%	2^{64}	[1]
	19	\mathcal{DD}	2+13+4	$2^{34.00}$	$2^{31.5}$	–	2^{64}	[7]
	21	\mathcal{DD}	4+13+4	$2^{55.25}$	$2^{31.0}$	–	2^{64}	[20]

1. \mathcal{DD} : differential distinguisher; \mathcal{ND} : differential-neural distinguisher; –: Not available;
2. *: 2.4 is the ratio of the time required for key recovery attacks using CPU and GPU in [3]; †: 2.92 is the ratio in our device.
3. We list two values of time complexity, $T_{\mathcal{ND}}$ and $T_{\mathcal{DD}}$. The $T_{\mathcal{ND}}$ is compared with \mathcal{ND} ; the $T_{\mathcal{DD}}$ is compared with \mathcal{DD} . For the reason for using two values of time complexity, please refer to Section 4.3.

input. The state of the next round (x_{i+1}, y_{i+1}) is computed as follows:

$$x_{i+1} := ((x_i \ggg 7) \boxplus y_i) \oplus k_i, y_{i+1} := (y_i \lll 2) \oplus x_{i+1}.$$

The round function (out of 32) of SIMON32/64 takes a 16-bit subkey k_i and a state consisting of two 16-bit words (x_i, y_i) as input. The next round state (x_{i+1}, y_{i+1}) is computed as follows:

$$x_{i+1} := (x_i \lll 1) \cdot (x_i \lll 8) \oplus (x_i \lll 2) \oplus y_i \oplus k_i, y_{i+1} := x_i.$$

119 2.2 The Model of Differential-Neural Distinguisher for SPECK32/64

120 The model of differential-neural distinguisher in [12,5,9] is almost identical except for the input. Thus, we introduce these models collectively. The differential-
121 neural distinguisher is a supervised model that distinguishes whether ciphertexts
122

123 are encrypted by plaintexts that satisfy a specific input difference or by random
 124 numbers. Given m plaintext pairs $\{(P_{i,0}, P_{i,1}), i \in [0, m - 1]\}$ and target cipher
 125 SPECK32/64, the resulting ciphertext pairs $\{(C_{i,0}, C_{i,1}), i \in [0, m - 1]\}$ are re-
 126 garded as an instance. Note that $m = 1$ in [12], $m \in \{1, 5, 10, 50, 100\}$ in [5], and
 127 $m \in \{2, 4, 8, 16\}$ in [9]. Each instance will be attached with a label Y :

$$Y = \begin{cases} 1, & \text{if } P_{i,0} \oplus P_{i,1} = \Delta, i \in [0, m - 1] \\ 0, & \text{if } P_{i,0} \oplus P_{i,1} \neq \Delta, i \in [0, m - 1] \end{cases}$$

128 where $\Delta = (0x0040, 0x0000)$. If Y is 1, this instance is sampled from the tar-
 129 get distribution and defined as a positive example. Otherwise, this instance is
 130 sampled from a uniform distribution and defined as a negative example. A large
 131 number of instances need to be trained in neural networks. when the neural
 132 network can obtain a stable accuracy higher than 0.5 on a test set, it can effec-
 133 tively distinguish whether ciphertexts are encrypted by plaintexts that satisfy a
 134 specific input difference or by random numbers. The model of differential-neural
 135 distinguisher can be described as:

$$\begin{aligned} \Pr(Y = 1 | X_0, \dots, X_{m-1}) &= F(f(X_0), \dots, f(X_{m-1}), \varphi(f(X_0), \dots, f(X_{m-1}))) \\ X_i &= (C_{i,0}, C_{i,1}), i \in [0, m - 1] \\ \Pr(Y = 1 | X_0, \dots, X_{m-1}) &\in [0, 1] \end{aligned}$$

136 where $f(X_i)$ represents the basic features of a ciphertext pair X_i , and $\varphi(\cdot)$ is the
 137 derived features, and $F(\cdot)$ is the new posterior probability estimation function.

138 The network architecture for training differential-neural distinguisher con-
 139 tains several modules described in Fig. 1. The input layer of the neural network
 140 consisting of multiple-ciphertext pairs is arranged in a $[m, \omega, \frac{2L}{\omega}]$ array, where
 141 L represents the block size of the target cipher, and ω is the size of a basic
 142 unit. For example, L is 32 and ω is 16 for SPECK32/64. Module 1 is the initial
 143 with-1 convolution layer that intends to make learning bit-sliced functions such
 144 as bitwise addition. Module 2 is the Residual Network. *Conv* stands for one-
 145 dimensional convolution *Conv1D* with $N_f = 32$ filters, and $k_s = 3$ is the size
 146 of the convolution kernel. The number of module 2 is determined by the exper-
 147 iment. The prediction head comprises modules 3, 4, and the output layer. *FC*
 148 is a fully connected layer that has $d_1 = 64$ or $d_2 = 64$ neurons. *BN* is the batch
 149 normalization layer. *Relu* and *Sigmoid* are two different activation functions.

150 2.3 Inception Network

151 Generally speaking, the safest way to improve network performance is to increase
 152 the width and depth of the network, which also has side effects. First, a deeper
 153 and wider network often means many parameters. When the amount of data is
 154 small, the trained network is easy to overfit, and when the depth of the network
 155 is deep, it is difficult to train and easy to cause greater errors. The two side
 156 effects of disappearance restrict the development of deep and wide convolutional
 157 neural networks, and the Inception network solves these two problems very well.

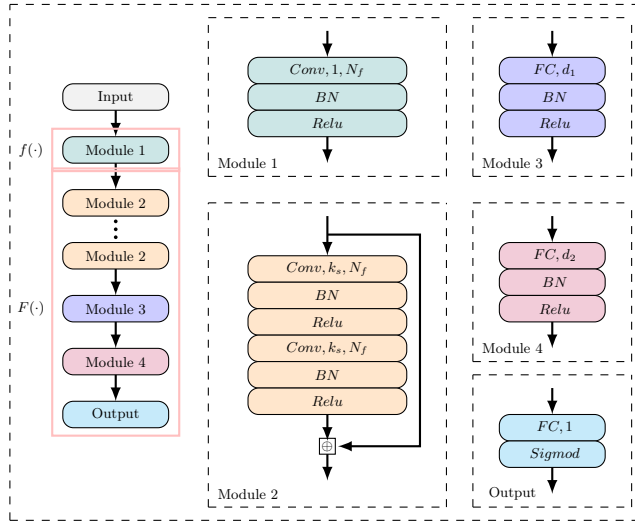


Fig. 1. The network architecture for training differential-neural distinguisher

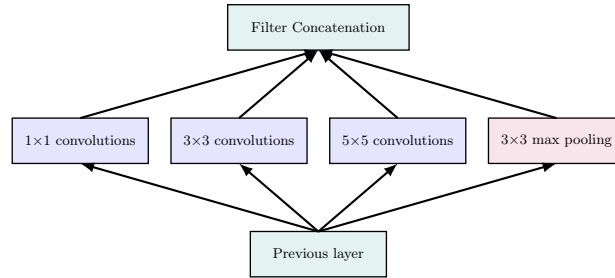
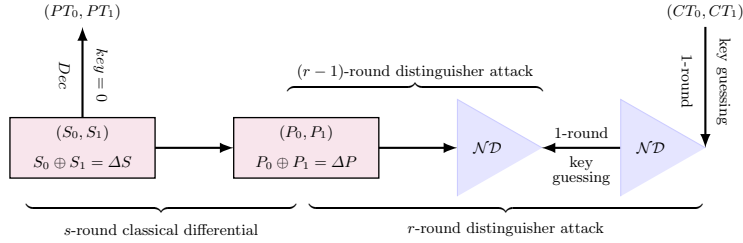


Fig. 2. Inception Module

158 One of the modules in the Inception network architecture is as follows in
 159 Fig. 2: in the same layer, there are 1×1 , 3×3 , 5×5 convolution and pooling
 160 layers, respectively, and the convolution operation and the pooling layer are
 161 pooled using filters. Padding is used in all operations to ensure that the output
 162 is the same size and the output results are all integrated after these operations.
 163 The feature of this module is that in the same layer, different features of the
 164 input of the previous layer are collected by using the above-mentioned filters of
 165 different sizes and performing pooling operations. This increases the width of the
 166 network and uses these different-sized filters and pooling operations to extract
 167 different features from the previous layer.

168 **2.4 Differential-neural Cryptanalysis**

 169 Gohr [12] proposed a framework for differential neural cryptanalysis dedicated to
 170 recovering the last two rounds of subkeys for SPECK. We decrypt the ciphertext
 171 using guessed subkey and use the differential-neural distinguisher to estimate
 172 the distance between the guessed subkey and the real key.

Fig. 3. $(1 + s + r + 1)$ -round key recovery attack of differential-neural cryptanalysis

 173 The overall processing of a key recovery attack based on the differential-
 174 neural distinguisher is shown in Fig. 3, where \mathcal{ND} is the trained differential-
 175 neural distinguisher, (PT_0, PT_1) is plaintext pairs and (CT_0, CT_1) is ciphertext
 176 pairs. The $(1 + s + r + 1)$ -round key recovery attack employs a r -round main
 177 and $(r - 1)$ -round helper differential-neural distinguisher trained using input
 178 pairs with difference ΔP . A short s -round classical differential ($\Delta S \rightarrow \Delta P$)
 179 with probability denoted by 2^{-p} is prepended on top of the differential-neural
 180 distinguisher to increase the number of the rounds of key recovery attack. To
 181 ensure the existence of data pairs satisfying the difference ΔP after s -round
 182 encryption, about $c \cdot 2^p$ (denoted by n_{cts}) data pairs with the difference ΔS
 183 are required according to the probability of difference propagation, where c is
 184 a small constant. Neutral bits of the s -round classical differential is used to ex-
 185 pand each data pair to a structure of n_b data pairs. The n_{cts} structures of the
 186 data pairs are decrypted in one round with 0 as the subkey to get the plain-
 187 text structures because the nonlinear operation occurs before the addition of
 188 keys for SPECK and SIMON. All plaintext structures are encrypted to obtain the
 189 corresponding ciphertext structures. Each ciphertext structure is used to select
 190 a candidate of the subkey by the r -round main differential-neural distinguisher
 191 based on a variant of Bayesian optimization. The usage of ciphertext structures
 192 is also highly selective by using a standard exploration-exploitation technique,
 193 namely *Upper Confidence Bounds*. Each ciphertext structure is assigned a priori
 194 according to the score of the recommended subkeys and the visited times.
 195 Without exhaustively performing trail decryption, the key search policy depends
 196 on the expected response of the differential-neural distinguisher upon wrong-key
 197 decryption. The *wrong key response profile* is to recommend new candidate val-
 198 ues from previous candidate values while minimizing the weighted Euclidean
 199 distance in a BAYESIANKEYSEARCH Algorithm [12].

200 2.5 Combined Response and Neutral Bits

201 As the number of encryption rounds increases, the accuracy of the differential-
 202 neural distinguisher decreases. To reduce the impact of the misjudgment of the
 203 single prediction of the distinguisher, Gohr used the combined response of the
 204 differential-neural distinguisher in ciphertext structure with the same distribu-
 205 tion, which can be satisfied by neutral bits [12]. The primary notion of neutral
 206 bits can be interpreted as follows.

207 **Definition 1 (Neutral bits of a differential, NB[6]).** Let $\Delta_{in} \rightarrow \Delta_{out}$ be
 208 a differential with input difference Δ_{in} and output difference Δ_{out} of a r -round
 209 encryption F^r . Let (P, P') be the input pair and $(C, C' \mid C = F^r(P), C' =$
 210 $F^r(P'))$ be the output pair, where $P \oplus P' = \Delta_{in}$. If $C \oplus C' = \Delta_{out}$, (P, P') is
 211 said to be conforming the differential $\Delta_{in} \rightarrow \Delta_{out}$. Let e_0, e_1, \dots, e_{n-1} be the
 212 standard basis of \mathbb{F}_2^n . Let i be an index of a bit (starting from 0). The i -th bit
 213 is a neutral bit for the differential $\Delta_{in} \rightarrow \Delta_{out}$, if $(P \oplus e_i, P' \oplus e_i)$ is also a
 214 confirming pair for any confirming pair (P, P') .

215 The responses $v_{i,k}$ from the differential-neural distinguisher on ciphertext
 216 pairs in the ciphertext structure (of size n_b) are combined using the Formula
 217 $s_k = \sum_{i=0}^{n_b-1} \log_2 \left(\frac{v_{i,k}}{1-v_{i,k}} \right)$ and s_k is used as the score of a recommended sub-
 218 key. The score s_k plays a decisive role in the execution time and success rate of
 219 the attack. The number of instances with the same distribution should be suffi-
 220 ciently large to enhance the distinguishing ability of the low-accuracy differential-
 221 neural distinguisher. However, neutral bits of the nontrivial classical differential
 222 are scarce. Therefore, probabilistic neutral bits (PNB) are exploited in [12].
 223 Some probabilistic neutral bits, simultaneous-neutral bit-sets (SNBS), condi-
 224 tional (simultaneous-) neutral bit(-set)s (CSNBS), and switching bits for adjoining
 225 differentials (SBfADs) were found in [3] (refer to Appendix A).

226 3 Differential-Neural Distinguishers for Round-Reduced 227 SPECK32/64

228 3.1 Network Architecture

229 The overall structure of our neural network for training the differential-neural
 230 distinguisher is depicted in Figure 4. Our neural network comprises four main
 231 components: an input layer that incorporates multiple ciphertext pairs, an initial
 232 convolutional layer consisting of four parallel convolutional layers, a residual
 233 tower that consists of multiple convolutional neural networks with two layers
 234 each, and a prediction head that comprises multiple fully connected layers.

235 **Input Representation.** When we have the output of the r -th round denoted as
 236 $(C, C') = (x_r \parallel y_r, x'_r \parallel y'_r)$, it can directly computes (y_{r-1}, y'_{r-1}) without knowl-
 237 edge of the $(r-1)$ -th subkey, using the round function of SPECK. Consequently,
 238 the neural network can process data in the format of $(x_r, x'_r, y_r, y'_r, y_{r-1}, y'_{r-1})$.

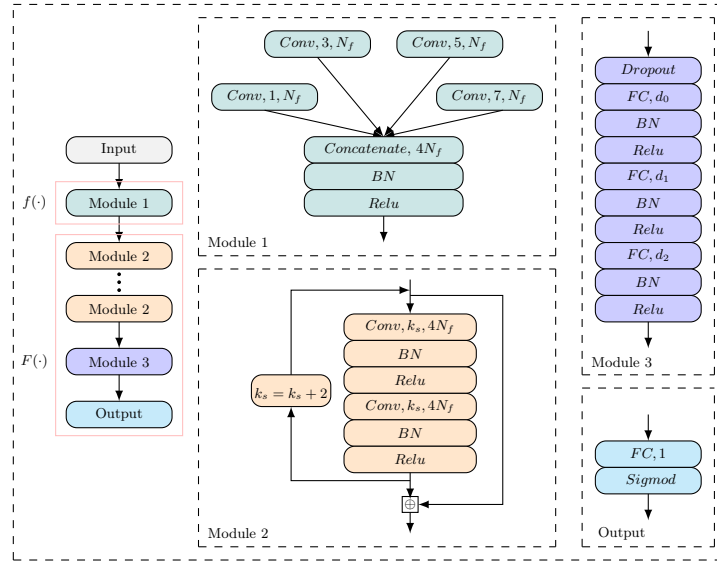


Fig. 4. The network architecture of our distinguisher for SPECK32/64

239 To accommodate this data format, the input layer of the neural network comprises
 240 m ciphertext pairs, where each pair consists of $3L$ units arranged in a
 241 $[m, \omega, \frac{3L}{\omega}]$ array. For SPECK32/64, the values of L and ω are set as 32 and 16
 242 respectively.

243 **Initial Convolution (Module 1).** The input layer is linked to the initial convo-
 244 lutional layer, which consists of four convolutional layers with $N_f = 32$ channels
 245 using various kernel sizes. Similar to GoogLeNet’s Inception [19], the outputs
 246 of the four convolutional layers are concatenated along the channel dimension.
 247 Batch normalization is applied to the concatenated outputs. Afterward, rectifier
 248 nonlinearity is applied to the batch normalized outputs, and the resulting matrix
 249 $[m, \omega, 4N_f]$ is then forwarded to the convolutional blocks layer.

250 **Convolutional Blocks (Module 2).** Each convolutional block consists of two
 251 layers of $4N_f$ filters. Each block applies first the convolution with kernel size
 252 $k_s = 3$, then a batch normalization, and finally a rectifier layer. At the end
 253 of the convolutional block, a skip connection is added to the output of the final
 254 rectifier layer of the block to the input of the convolutional block. It transfers the
 255 result to the next block. After each convolutional block, the kernel size increases
 256 by 2. The number of convolutional blocks is 5 in our model (determined by
 257 experiment).

258 **Prediction Head (Module 3 and Output).** The prediction head consists
 259 of three hidden layers and one output unit. Before the first hidden layer, we
 260 add a dropout layer to prevent model overfitting. The three fully connected

261 layers comprise $d_0 = 512$, $d_1 = 64$, and $d_2 = 64$ units, followed by the batch
 262 normalization and rectifier layers. The final layer consists of a single output unit
 263 using the activation function *Sigmoid*.

264 **Rationale.** Firstly, we make adjustments to the model’s input data format. By
 265 utilizing the ciphertext from the last round, we can calculate the right half of
 266 the penultimate round’s ciphertext without knowledge of the $(r-1)$ -th subkey,
 267 using the round function of SPECK32/64. Second, considering the cyclic shift
 268 operation and modulo addition in the round function, we introduce convolution
 269 operations with widths of 3, 5, and 7 to try to capture the information that may
 270 exist in adjacent bits. This allows us to capture multidimensional features, tak-
 271 ing inspiration from the Inception block in GoogLeNet[19]. Thirdly, to enhance
 272 the receptive field of the convolutions, we increase the size of the convolutional
 273 kernels by 2 as the Residual Network’s depth grows. The size of the convolution
 274 kernel is increased by 2 each time to ensure that the size of the convolution layer
 275 is an odd number. Additionally, we incorporate a dropout layer before the fully
 276 connected layer to enhance the network’s generalization ability.

277 3.2 The Training of Differential-Neural Distinguisher

278 The accuracy serves as the paramount metric to evaluate the performance of
 279 the differential-neural distinguisher. Subsequently, the subsequent training pro-
 280 cedure was conducted to validate the efficacy of our network architecture.

281 **Data Generation.** Training and test sets were generated using the Linux ran-
 282 dom number generator to obtain uniformly distributed keys K_i and multiple-
 283 plaintext pairs $\{(P_{i,j,0}, P_{i,j,1}), j \in [0, m - 1]\}$ with the input difference $\Delta =$
 284 $(0x0040, 0x0000)$ and a vector of binary-valued labels Y_i . During the production
 285 of training or test sets for r -round SPECK32/64, the multiple-plaintext pairs
 286 were then encrypted for r rounds if $Y_i = 1$, while otherwise, the second plaintext
 287 of the pairs was replaced with a freshly generated random plaintext and then
 288 encrypted for r rounds.

289 *Remark 1.* We use two different numbers of datasets to train differential-neural
 290 distinguisher. In [12], the training and test sets include N and M instances,
 291 consisting of a ciphertext pair in an instance, total N and M ciphertext pairs,
 292 respectively. In [9], the training set and test set include N/m and M/m instances,
 293 and each instance includes m ciphertext pairs; that is, the total numbers of
 294 ciphertext pairs used are N and M . To ensure a fair comparison, we used N/m
 295 and M/m instances as training and test sets. However, it may lead to overfitting
 296 (see Remark 2 for details). To overcome this problem, we also use N and M
 297 instances as training test and test set, which consists of m ciphertext pair, that
 298 is, total $N \times m$ and $M \times m$ ciphertext pairs, respectively.

299 **Basic Training Scheme.** We conducted the training for 20 epochs in the
 300 dataset for $N = 10^7$ and $M = 10^6$. The batch size processed by the dataset

301 is adjusted according to the parameter m to maximize GPU performance. Op-
 302 timization was performed against mean square error loss plus a small penalty
 303 based on L2 weights regularization parameter $c = 10^{-5}$ using the Adam algo-
 304 rithm [17]. A cyclic learning rate schedule was applied, setting the learning rate
 305 l_i for epoch i to $l_i = \alpha + \frac{(n-i) \bmod (n+1)}{n} \cdot (\beta - \alpha)$ with $\alpha = 10^{-4}$, $\beta = 2 \times 10^{-3}$
 306 and $n = 9$. The networks obtained at the end of each epoch were stored, and
 307 the best network by validation loss was evaluated against a test set.

308 **Training (8-9)-round Distinguishers Using Staged Train Method.** We
 309 use several stages of pretraining to train an 8-round differential-neural distin-
 310 guisher for SPECK32/64. First, we use our 7-round distinguisher to recognize
 311 5-round SPECK32/64 with the input difference (0x8000, 0x804a) (the most likely
 312 difference to appear three rounds after the input difference (0x0040, 0x0000)).
 313 The training was done in 10^7 instances for 20 epochs with a learning rate of
 314 10^{-4} . Then we trained the distinguisher to recognize 8-round SPECK32/64 with
 315 the input difference (0x0040, 0x0000) by processing 10^7 freshly generated in-
 316 stances for 10 epochs with a learning rate of 10^{-4} . Finally, the learning rate
 317 was reduced to 10^{-5} after processing another 10^7 new instances for 10 epochs.
 318 For the 9-round distinguisher, the overall training method is the same. The only
 319 difference is the use of an 8-round distinguisher to identify 5-round SPECK32/64
 320 with the input difference (0x850a, 0x9520) (the most likely difference to appear
 321 four rounds after the input difference (0x0040, 0x0000)).

322 3.3 Result

323 **Test Accuracy.** We summarize the accuracy of 6, 7, 8-, and 9-round differential-
 324 neural distinguisher compared to [12,9,5] in Table 2. Also, we list the accuracy
 325 (Acc), the true positive rate (TPR), and the true negative rate (TNR) tested on
 326 newly generated data in Table 3. The 6, and 7-round distinguishers were trained
 327 using the basic training method, while the 8, and 9-round distinguishers were
 328 trained using the staged training method. If the accuracy is greater than 0.5,
 329 it is considered effective. The “ N/m ” column results in accuracy using N/m and
 330 M/m instances as training and test sets, respectively. The “ N ” column results
 331 from accuracy using N and M instances as the training and test sets, respec-
 332 tively. From Table 2, the accuracy of our differential-neural distinguisher was
 333 significantly improved in both the “ N/m ” column and the “ N ” column compared
 334 to [13,9,5]. There are some differences in accuracy under the two experiments
 335 caused by overfitting of the model; see *Remark 2* for details.

336 In Table 2, except for Benamira’s result [5], other results are directly trained
 337 by the neural network. In [5], the value of m is $\{1, 5, 10, 50, 100\}$. But in order
 338 to facilitate the key recovery attack, we set the value of m at the power of
 339 2, that is, $\{2, 4, 8, 16\}$. When $m = 1$, the case of Benamira and Gohr is the
 340 same. In [5], they use two ways to train and evaluate the differential-neural
 341 distinguisher with multiple ciphertext pairs. The straightforward one (Averaging
 342 Method) is to evaluate the neural distinguisher score for each element of the

Table 2. Summary accuracy of distinguisher on SPECK32/64 using different number of instances

r	$m=2$				$m=4$				$m=5$		
	[9]	[13]*	N/m	N	[9]	[13]*	N/m	N	[5]	N/m	N
6	0.8613	0.877	0.8771	0.8773	0.931	0.950	0.9468	0.9497	0.9541	0.9623	0.965
7	0.6393	0.663	0.6663	0.6649	0.6861	0.725	0.7194	0.7283	0.735	0.7436	0.7491
8	-	0.521	-	-	-	0.530	0.5329	0.5428	-	-	-
r	$m=8$				$m=10$			$m=16$			
	[9]	[13]*	N/m	N	[5]	N/m	N	[9]	[13]*	N/m	N
6	0.9562	0.990	0.9868	0.9895	0.99	0.9915	0.9939	0.9802	1.000	0.9969	0.9992
7	0.7074	0.801	0.7991	0.8106	0.808	0.8243	0.8341	0.6694	0.883	0.8759	0.8963
8	-	0.543	0.5347	0.5590	-	-	-	-	0.560	0.5566	0.5854
9	-	-	-	0.5024	-	-	-	-	-	-	0.5050

1. *: combining the scores of multiple distinguishers trained by using single-ciphertext pair under independence assumption.

Table 3. Acc, TPR, TNR of distinguisher on SPECK32/64 using N instances

m	r	Acc	TPR	TNR	m	r	Acc	TPR	TNR
	6	0.8768	0.8448	0.9087	6	6	0.9495	0.9429	0.9559
2	7	0.6635	0.6240	0.7029	4	7	0.7291	0.7048	0.7532
	8	-	-	-	8	8	0.5428	0.5318	0.5537
	6	0.9897	0.9862	0.9931	6	6	0.9992	0.9988	0.9996
8	7	0.8103	0.8024	0.8184	16	7	0.8958	0.8906	0.9009
	8	0.5562	0.5434	0.5690	8	8	0.5853	0.5704	0.6002
	9	0.5016	0.2122	0.7915	9	9	0.5045	0.5175	0.4915

343 multiple ciphertext pairs and then take the results' median. The second (2D-
 344 CNN Method) is to consider the whole multiple ciphertext pairs as a single
 345 input for a neural network. These two methods are theoretically equivalent,
 346 but the second method to train the differential-neural distinguisher will have
 347 lower accuracy. Benamira use two methods to get the accuracy of the 6-round
 348 distinguisher. When $m = 5$, the accuracy of the two methods is 0.9541 and
 349 0.9327, respectively; When $m = 10$, the accuracy of the two methods is 0.99
 350 and 0.977, respectively, in [5]. We can see that the accuracy of the distinguisher
 351 obtained by the second method is lower than that of the first method. However,
 352 the accuracy of the 7-round distinguisher is obtained by the first method in [5].
 353 This means the accuracy obtained should be even lower if the distinguisher is
 354 trained directly using a neural network.

355 *Remark 2. Why do we train a differential-neural distinguisher with two different*
 356 *numbers of data?* For the sake of fairness of comparison, we must use N/m and
 357 M/m instances as training and test sets (see *Remark 1*). However, from Fig. 5a,
 358 we can see that the difference between training and test accuracy is relatively
 359 significant. In other words, using N/m and M/m instances as training and test
 360 set to train a neural network will suffer overfitting, especially when the number
 361 of rounds r and m is large. For more overfitting phenomena, please refer to
 362 Appendix C. However, the training and test accuracy are almost equal in Fig. 5b.
 363 Therefore, using N and M instances as the training set and a test set to train
 364 the differential-neural distinguisher can avoid overfitting, speed up the model
 365 convergence, and improve the model accuracy to a certain extent. Due to the
 366 overfitting phenomenon, the accuracy of the distinguisher will be low, which also
 367 affects our training of more rounds of differential-neural distinguisher.

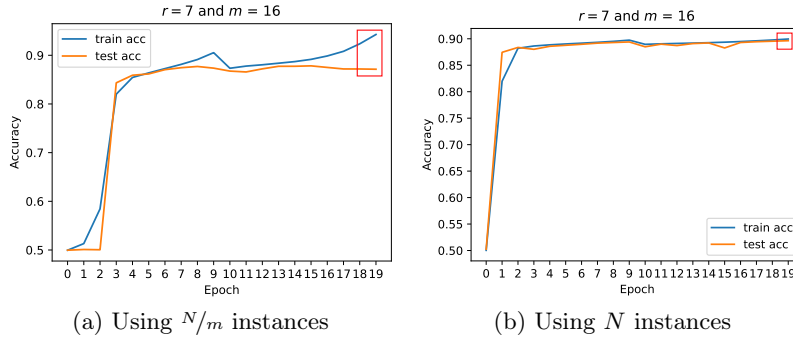


Fig. 5. Overfitting with the different number of instances.

368 **Wrong Key Response Profile.** The key search policy depends on an impor-
 369 tant observation that the expected response of the distinguisher upon wrong-key
 370 decryption will rely on the bitwise difference between the guessed subkey and the
 371 real subkey. The *wrong key response profile*, which is precomputed by using 3000
 372 ciphertext pairs for each guessed subkey, is used to recommend new candidate
 373 values for the key from previous candidate values by minimizing the weighted
 374 Euclidean distance as the criteria in a BAYESIANKEYSEARCH Algorithm. It recom-
 375 mends a set of subkeys and provides their scores without exhaustively per-
 376 forming the trial decryption. The μ and δ represent the empirical mean and
 377 standard deviation of the distinguisher score over these 3000 ciphertext pairs.

378 The abscissa in Fig. 6 and 7 is the difference between the guessed subkey and
 379 the real subkey, and the ordinate is the score obtained by putting the ciphertext
 380 pairs obtained after decrypting multiple ciphertext pairs (encrypted with the
 381 same key) with the guessed subkey into the differential-neural distinguisher. If
 382 the Hamming weight of the difference between guessed and real subkey is small,
 383 the distinguisher will score high; otherwise, the score will be low. From Fig. 6

384 and 7, we can see that when the Hamming weight of the key difference is small,
 385 our differential-neural distinguisher scores higher than that of the Gohr’s distin-
 386 guisher in the same abscissa. We can get lower scores when the Hamming weight
 387 is larger. In other words, our distinguisher is better able to judge the Hamming
 388 distance between the real subkey and the guessed subkey, thus recommending
 389 candidate subkeys that are closer to the real subkey.

390 Moreover, it can be observed that the score of the distinguisher is higher when
 391 the difference between the guessed key and the real key belongs to $\{16384, 32768,$
 392 $49152\}$, where the vertical coordinates of "*" correspond to these positions. This
 393 means that when the 14th and 15th bits of the subkey are guessed incorrectly,
 394 it has little effect on the score of the distinguisher. Therefore, it is possible to
 395 reduce the key guessing space by not guessing these two bits, and this feature is
 396 also used in [12] to accelerate the key recovery attack.

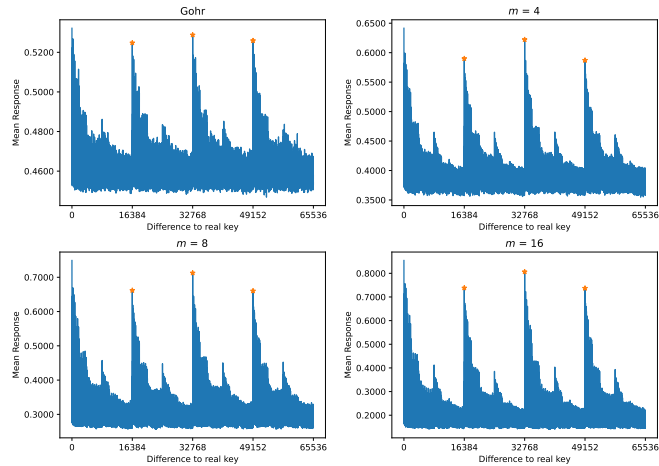


Fig. 6. Wrong key response profile for 7-round SPECK32/64 using N instances

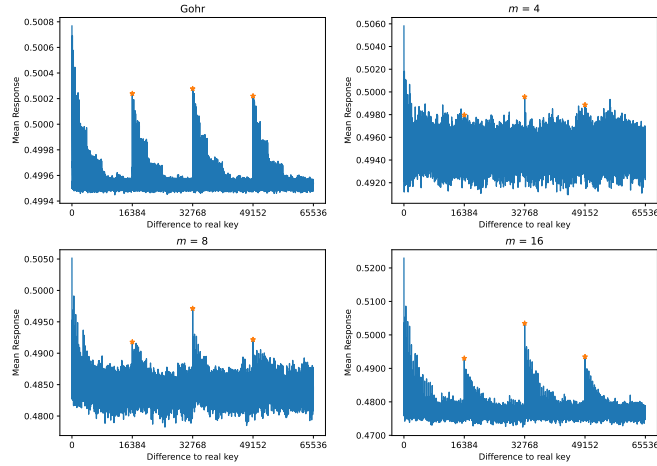


Fig. 7. Wrong key response profile for 8-round SPECK32/64 using N instances

397 4 From Differential-Neural Distinguisher to Key 398 Recovery Attack

399 4.1 Generation of Same Distributed Data

400 During the training of the differential-neural distinguisher, we take multiple ci-
401 phertext pairs as an instance and then put the instance into the neural network.
402 In the positive example, we require multiple ciphertext pairs of an instance to
403 be obtained by encrypting multiple plaintext pairs satisfying the same difference
404 Δ_P .

405 After obtaining a differential-neural distinguisher, we add a classical differen-
406 tial $\Delta_S \rightarrow \Delta_P$ before the differential-neural distinguisher to increase the number
407 of rounds for the key recovery attack. However, the classical differential is proba-
408 bilistic. During the key recovery attack, even if multiple plaintext pairs have the
409 same difference Δ_S of an instance, the difference between multiple ciphertext
410 pairs of an instance may not be the same after propagation through the classical
411 differential. We need to take certain measures to make the multiple ciphertext
412 pairs of an instance have the same difference after the classical difference prop-
413 agation.

414 Neutral bits can solve the problem of obtaining multiple ciphertext pair that
415 satisfies the same difference after propagation through the classical differential,
416 ensuring we can launch key recovery attacks. We randomly generate a plaintext
417 pair satisfying the initial difference Δ_S and flip the ciphertext bits correspond-
418 ing to $\log_2 m$ neutral bits to obtain m plaintext pairs. The m ciphertext pairs
419 obtained by the propagation of the m plaintext pairs through the classical dif-
420 ferential have the same difference.

4.2 Experimental Environment and Data Complexity

Following to the settings in [12], we count a key guess as successful if the last round key was guessed correctly and the second round key is at the hamming distance at most two of the real key. The experiment is conducted by Python 3.7.15 and Tensorflow 2.5.0 in Ubuntu 20.04. The device information is Intel(R) Xeon(R) Gold 6226R*2 with 2.90GHz, 256GB RAM, and NVIDIA RTX2080Ti 12GB*5. In our implementation, the performance is not constrained by the speed of neural network evaluation when using a high-performance graphics card. Instead, the total number of iterations on the ciphertext structures determines the limiting factor. The experimental parameters for key recovery attacks are denoted below.

1. n_{kg} : the number of times to guess the subkey k_r involved in the condition.
2. n_{cts} : the number of ciphertext structure.
3. n_b : the number of ciphertext pairs in each ciphertext structure, that is, $2^{|NB|}$.
4. n_{it} : the total number of iterations on the ciphertext structures.
5. c_1 and c_2 : the cutoffs with respect to the scores of the recommended last subkey and second to last subkey, respectively.
6. n_{byit1}, n_{cand1} and n_{byit2}, n_{cand2} : the number of iterations and the number of key candidates within each iteration in the BAYESIANKEYSEARCH Algorithm to guess each of the last and the second to last subkeys, respectively.

Theoretical Data Complexity. During a key recovery attack, the classical differential or neutral bits used may need to satisfy some conditions involving the key. The data complexity of the experiment is calculated using the formula $n_{kg} \times n_b \times n_{ct} \times m \times 2$. The data complexity is calculated as theoretical values. In the actual experiment, when the accuracy of the differential-neural distinguisher is high, the key can be recovered quickly and successfully. Not all the data is used, so the actual data complexity is lower than the theoretical.

4.3 Experimental Time Complexity.

How to reasonably calculate the time complexity and compare it fairly with previous work has always been a difficult task.

- In classical differential cryptanalysis, researchers usually calculate the number of full encryption (the number of rounds of attack) required to perform a key recovery attack as the time complexity of the attack [10,1,7,11,8].
- In differential-neural cryptanalysis, Gohr[12] uses GPU to train differential-neural distinguisher but uses CPU to implement key recovery attacks. Therefore, he estimates that a highly optimized, fully SIMD-parallelized implementation of SPECK32/64 could perform brute force key search at a speed of about 2^{28} keys per second per core. Later, Bao [3] *et al.* used GPU to accelerate key recovery attacks for 13-round SPECK32/64. For a fair comparison with previous

work, they also used 2^{28} as the benchmark for encryption speed and estimated the ratio ($\text{Ratio}_{cpu/gpu}$) of the time required for key recovery attacks using CPU and GPU, where $\text{Ratio} = 2^{2.4}$ in [3].

To ensure a fair comparison, we conduct multiple key recovery attacks and determine the average running time (rt) as the representative time for each experiment. Additionally, we compute the success rate (sr) of the key recovery attack by dividing the number of successful experiments by the total number of experiments conducted. In addition, classical differential cryptanalysis methods all use the CPU to execute key recovery attack programs. Part of the program of the key recovery attack of differential-neural cryptanalysis needs to be executed by GPU. For a fairer comparison, we conducted several experiments to calculate the ratio of the time required to perform key recovery attacks using CPU and GPU in our device. The specific results are shown in Table 4.

Table 4. Calculate the ratio of time required for key recovery attack using CPU and GPU

R	Conf.	c_1	c_2	n_{cts}	n_{it}	N_e	Device	rt	$\text{Ratio}_{cpu/gpu}$	sr	Ref.
11	1+2+7+1	5	10	100	500	100	CPU	299.26	$2^{0.39}$	53%	[12]
							GPU	227.05		51%	[12]
12	1+3+7+1	7	10	2^{11}	2^{12}	40	CPU	4272.91	$2^{2.92}$	100%	This work
							GPU	564.67		100%	This work

From Table 4, we can see that the ratio of the time required for the key recovery attack on 11 rounds of speck32/64 using the distinguisher trained by Gohr [12] on the CPU and GPU is $2^{0.39}$. When performing a key recovery attack on 12-round speck32/64 using our trained distinguisher, the ratio is $2^{2.92}$. We choose the maximum value of the two ratios $2^{2.92}$ as the final value of $\text{Ratio}_{cpu/gpu}$. According to different attack methods, we give two different time complexity calculation methods.

- **Comparison with Differential-neural Cryptanalysis:** We follow the setting of Gohr [12] and Bao [3] et al. to calculate the time complexity of the key recovery attack. we used 2^{28} as the benchmark for encryption speed. Then the calculation formula of time complexity T_{ND} is $n_{kg} \times rt \times 2^{28} \times 2^{2.92}$.
- **Comparison with Classical Differential Cryptanalysis:** we utilize a 2^{32} plaintext to evaluate our device's encryption speed E_s . For SPECK32/64, each core can execute approximately $2^{27.09}$ 1-round encryption per second, i.e., $E_s = 2^{27.09}$; For SIMON32/64, each core can execute approximately $2^{25.48}$ 1-round encryption per second, i.e., $E_s = 2^{25.48}$. Then the calculation formula of time complexity T_{DD} is $n_{kg} \times rt \times \frac{E_s}{R} \times 2^{2.92}$, where R is the number of rounds for key recovery attack.

491 5 Key Recovery Attack on Round-Reduced SPECK32/64

492 In this section, we demonstrate the effectiveness of our differential-neural distin-
 493 guisher in enhancing the performance of key recovery attacks. We adopt a similar
 494 framework as described in previous works [12,3], with the key difference being
 495 the utilization of the differential-neural distinguisher trained on N instances.
 496 For a more complete key recovery attack procedure, please refer to Appendix B.
 497 We have successfully reduced the time and data complexity of 13-round key
 498 recovery attacks for SPECK32/64 by employing an improved differential-neural
 499 distinguisher. Moreover, we leverage the outcomes of the 13-round key recovery
 500 attack to estimate the complexity involved in a 14-round key recovery attack.

501 5.1 Key Recovery Attack on 13-round SPECK32/64

502 Combining a 3-round classical differential with an 8-round differential-neural dis-
 503 tinguisher, we examine how far a practical attack can go on 13-round SPECK32/64
 504 in this subsection.

505 **Experiment 1:** The components of key recovery attack $\mathcal{A}_I^{\text{SPECK13R}}$ of 13-
 506 round SPECK32/64 are shown as follows.

- 507 1. 3-round classical differential $(0x8020, 0x4101) \rightarrow (0x0040, 0x0000)$;
- 508 2. generalized neutral bits of generating multiple-ciphertext pairs: $\{[22], [20],$
 509 $[13]\}$; generalized neutral bits of combined response of differential-neural dis-
 510 tinguisher: $\{[5, 28], [15, 24], [12, 19], [6, 29], [6, 11, 12, 18], [4, 27, 29], [14, 21], [0, 8,$
 511 $31], [30]\}$ (refer to Table 10).
- 512 3. 8-round differential-neural distinguisher $\mathcal{ND}^{\text{SPECK}_{8r}}$ under difference $(0x0040,$
 513 $0x0000)$ and its wrong key response profiles $\mathcal{ND}^{\text{SPECK}_{8r}} \cdot \mu$ and $\mathcal{ND}^{\text{SPECK}_{8r}} \cdot \delta$.
- 514 4. 7-round differential-neural distinguisher $\mathcal{ND}^{\text{SPECK}_{7r}}$ under difference $(0x0040,$
 515 $0x0000)$ and its wrong key response profiles $\mathcal{ND}^{\text{SPECK}_{7r}} \cdot \mu$ and $\mathcal{ND}^{\text{SPECK}_{7r}} \cdot \delta$.

516 In the beginning, we guess three key bits of k_0 , that is $k_0[7]$, $k_0[5] \oplus k_0[14]$,
 517 and $k_0[15] \oplus k_0[8]$ because of the 3-round differential (refer to Table 9) and
 518 four key bits $k_0[12] \oplus k_0[5]$, $k_0[1]$, $k_0[2] \oplus k_0[11]$, $k_0[11] \oplus k_0[4]$ to employ four
 519 conditional neutral bits (refer to Table 10). Thus, n_{kg} is 2^7 . However, to make
 520 the experimental verification economic, we tested the core of the attack with
 521 the seven conditions being fulfilled only. The concrete parameters used in our
 522 13-round key recovery attack $\mathcal{A}^{\text{SPECK13R}}$ are listed below.

$n_{kg} = 2^7$	$m = 8$	$n_b = 2^9$	$n_{cts} = 2^{11}$
$n_{it} = 2^{12}$	$c_1 = 5, c_2 = -86$	$n_{byit1} = n_{byit2} = 5$	$n_{cand1} = n_{cand2} = 32$

524 Because the prepended classical differential is valid when the keys fulfil
 525 $k_2[12] \neq k_2[11]$, we tested only for these valid keys, and the presented at-
 526 tack works for 2^{63} keys. The data complexity is $2^7 \times 2^9 \times 2^{11} \times 8 \times 2 = 2^{31}$
 527 plaintexts. The core of the attack was examined in 100 trials; there are 41 suc-
 528 cessful trials, that is, $sr = 41\%$. The average run time of every trail in our
 529 server is 15223.20s. Thus, the time complexity $T_{\mathcal{ND}} = n_{kg} \times rt \times 2^{28} \times 2^{2.92} =$
 530 $2^7 \times 15223.21 \times 2^{28} \times 2^{2.92} = 2^{48.89+2.92}$; $T_{\mathcal{DD}} = n_{kg} \times rt \times \frac{E_s}{R} \times 2^{2.92} =$
 531 $2^7 \times 15223.21 \times \frac{2^{27.09}}{13} \times 2^{2.92} = 2^{44.28+2.92}$.

532 **5.2 Using Two Classical Differentials and SBfADs for 13-round**
 533 **SPECK32/64**

534 Bao *et al.* found that the output of the classical differential matters to the
 535 differential-neural distinguisher but not the input difference. Hence, more than
 536 one differential can be prepended to a differential-neural distinguisher if they
 537 share the same output difference. Multiple such classical differentials can share
 538 some neutral bits. Using such classical differentials might enable data reuse, thus
 539 slightly reducing data complexity. Also, they employ SBfADs to save one guessed
 540 key bit and reduce time and data complexity by half compared to the CSNBS. To
 541 further exploit the capabilities of our differential-neural distinguisher, we again
 542 implement a 13-round key recovery attack using two classical differentials and
 543 SBfADs.

544 **Experiment 2:** The components of key recovery attack $\mathcal{A}_{II}^{\text{SPECK}13R}$ of 13-
 545 round SPECK32/64 are shown as follows.

- 546 1. 3-round classical differentials $(0x8020, 0x4101) \rightarrow (0x0040, 0x0000)$ and $(0x80$
 547 $60, 0x4101) \rightarrow (0x0040, 0x0000)$;
- 548 2. generalized neutral bits of generating multiple-ciphertext pairs: $\{[20], [13], [12,$
 549 $19]\}$; generalized neutral bits of combined response of differential-neural distin
 550 guisher: $\{[22], [14, 21], [6, 29], [30], [0, 8, 31], [5, 28], [15, 24], [4, 27, 29]\}$ (refer to
 551 Table 10 and one SBfADs [21]).
- 552 3. 8-round differential-neural distinguisher $\mathcal{ND}^{\text{SPECK}_{8r}}$ under difference $(0x0040,$
 553 $0x0000)$ and its wrong key response profiles $\mathcal{ND}^{\text{SPECK}_{8r}} \cdot \mu$ and $\mathcal{ND}^{\text{SPECK}_{8r}} \cdot \delta$.
- 554 4. 7-round differential-neural distinguisher $\mathcal{ND}^{\text{SPECK}_{7r}}$ under difference $(0x0040,$
 555 $0x0000)$ and its wrong key response profiles $\mathcal{ND}^{\text{SPECK}_{7r}} \cdot \mu$ and $\mathcal{ND}^{\text{SPECK}_{7r}} \cdot \delta$.

556 In the beginning, we only guess two key bits of k_0 , that is, $k_0[7]$ and $k_0[15] \oplus k_0[8]$
 557 because of two 3-round classical differentials and two key bits $k_0[12] \oplus k_0[5]$, $k_0[1]$
 558 to employ two CSNBS (refer to Table 10). Because we use two classical differ-
 559 entials $(0x8020, 0x4101) \rightarrow (0x0040, 0x0000)$ and $(0x8060, 0x4101) \rightarrow (0x0040,$
 560 $0x0000)$, the condition $k_0[5] \oplus k_0[14]$ is unnecessary (refer to Table 9). Besides,
 561 we use SBfADs [21] instead of CSNBS [6, 11, 12, 18], the key bit $k_0[2] \oplus k_0[11]$
 562 does not need to be guessed. Note that although we used SNBS [4, 27, 29], we
 563 did not use key condition $k_0[11] \oplus k_0[4]$ to increase its probability, because 0.672
 564 is already high enough. Thus, $n_{kg} = 2^4$. However, to make the experimental
 565 verification economic, we tested the core of the attack with the four conditions
 566 being fulfilled only. The concrete parameters used in our 13-round key recovery
 567 attack $\mathcal{A}_{II}^{\text{SPECK}13R}$ are listed below.

$n_{kg} = 2^4$	$m = 8$	$n_b = 2^{8+1}$	$n_{cts} = 2^{11}$
$n_{it} = 2^{12}$	$c_1 = 8, c_2 = -500$	$n_{byit1} = n_{byit2} = 5$	$n_{cand1} = n_{cand2} = 32$

569 Because the prepended classical differential is valid when the keys fulfill
 570 $k_2[12] \neq k_2[11]$, we tested only for these valid keys, and the presented attack
 571 works for 2^{63} keys. The data complexity is $2^4 \times 2^9 \times 2^{11} \times 8 \times 2/2 = 2^{27}$ plaintexts.
 572 Note that the data complexity is divided by 2 because if we use two classical dif-
 573 ferences, one can generate half of the required data pairs for free. The core of the

574 attack was examined in 100 trials; there are 21 successful trials, that is, $sr = 21\%$.
 575 The average run time of every trail in our server is 17011.22s. Thus, the time
 576 complexity $T_{\mathcal{ND}} = n_{kg} \times rt \times 2^{28} \times 2^{2.92} = 2^4 \times 17011.22 \times 2^{28} \times 2^{2.92} = 2^{46.05+2.92}$;
 577 $T_{\mathcal{DD}} = n_{kg} \times rt \times \frac{E_s}{R} \times 2^{2.92} = 2^4 \times 17011.22 \times \frac{2^{27.09}}{13} \times 2^{2.92} = 2^{41.44+2.92}$.

578 5.3 Brute Force Guessing of 1-round Subkey for 14-round 579 SPECK32/64

580 Under the current framework, there are two ways to increase the number of
 581 rounds of key recovery attacks. One is to increase the length of the classical
 582 differential, and the other is to increase the length of the difference-neural dis-
 583 tinguisher, but it seems that these two paths are not feasible under the current
 584 results.

585 - **Increase the Length of the Classical Differential.** In the 13-round key
 586 recovery attack, the probability of the 3-round sub-optimal classical differ-
 587 entials we use is 2^{-12} , and the complexity of the core attack is about $2^{42.07}$.
 588 We use the MILP model to search for 4-round optimal classical differential
 589 path $(0x1488, 0x1008) \rightarrow (0x0040, 0x0000)$ with a probability of 2^{-17} . When
 590 we use a 4-round classical differential to implement a 14-round key recovery
 591 attack, the time complexity of the core attack will exceed 2^{47} under ideal
 592 circumstances, which is beyond our current computing equipment. Also, the
 593 4-round classical differential doesn't have enough neutral bits to use for key
 594 recovery attacks.

595 - **Increase the Length of the Differential-neural Distinguisher.** Al-
 596 though we trained a 9-round differential-neural distinguisher, its accuracy
 597 was too low, and we can not implement a 14-round key recovery attack.
 598 According to our calculations, the accuracy of DDT should be 0.5089 and
 599 0.5138 in the case of $m = 8$ and $m = 16$, respectively. In addition, it has
 600 been proved that the differential-neural distinguisher can learn more features
 601 than DDT, so the accuracy of the differential-neural distinguisher should be
 602 higher than that of DDT. Suppose we can further improve the accuracy of
 603 the 9-round differential-neural distinguisher. In that case, it will be possible
 604 to directly implement a 14-round key recovery attack, which we will continue
 605 to study.

606 Fortunately, we can estimate the time complexity of a 14-round key recovery
 607 attack. Notably, the time complexity for our 13-round key recovery attack is suf-
 608 ficiently low. By employing a brute force approach to guess one round of subkey,
 609 we can subsequently execute a 14-round key recovery attack. The time complex-
 610 ity of the 14-round attack is determined by multiplying the time complexity of
 611 the 13-round attack by 2^{16} . According to two different complexity calculation
 612 formulas, we can give the time complexity of the 14-round key recovery attack.

- 613 1. The time complexity $T_{\mathcal{ND}} = 2^{16} \times n_{kg} \times rt \times 2^{28} \times 2^{2.92} = 2^{16} \times 2^4 \times 17011.22 \times$
 614 $2^{28} \times 2^{2.92} = 2^{62.05+2.92}$. Note that this time complexity exceeds that of brute
 615 force key search.

616 2. The time complexity $T_{DD} = 2^{16} \times n_{kg} \times rt \times \frac{E_s}{R} \times 2^{2.92} = 2^{16} \times 2^4 \times 17011.22 \times$
 617 $\frac{2^{27.09}}{13} \times 2^{2.92} = 2^{57.44+2.92}$.

618 **6 Differential-Neural Distinguishers on Round-Reduced**
 619 **SIMON32/64**

620 In ASIACRYPT 2022, Bao *et al.* used the Dense Network and Squeeze-and-
 621 Excitation Network to train 9, 10, and 11-round differential-neural distinguish-
 622 ers for SIMON32/64 [3]. We give the accuracy of the 9, 10, 11, and 12-round
 623 differential-neural distinguisher for SIMON32/64 using modified network archi-
 624 tecture in case of multiple ciphertext pairs.

625 **6.1 Network Architecture**

626 The network architecture of the differential-neural distinguisher used to train
 627 SIMON32/64 is generally similar to that of SPECK32/64. Based on the round
 628 function of SIMON32/64, we modify the number of convolutional layers and the
 629 size of the convolutional kernel in the Inception module and use a GlobalAver-
 630 agePooling layer instead of three fully connected layers. The overall architecture
 631 is shown in Fig 8.

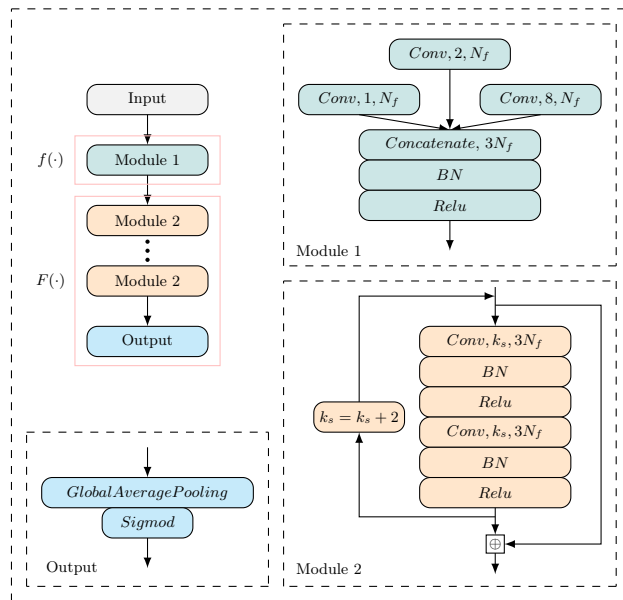


Fig. 8. The network architecture of our distinguisher for SIMON32/64

632 **Input Representation.** Based on the round function, $(y_{r-1} \oplus y'_{r-1})$ can be
 633 obtained without knowing the $(r-1)$ -th subkey for SIMON32/64. Thus, the neural
 634 network accepts data of the form $(x_r, x'_r, y_r, y'_r, y_{r-1} \oplus y'_{r-1})$. The input layer has
 635 m ciphertext pairs consisting of $2.5L$ units likewise arranged in a $[m, \omega, \frac{2.5L}{\omega}]$
 636 array, where $L = 32, \omega = 16$ for SIMON32/64.

637 **Initial Convolution (Module 1).** The input layer is connected to the initial
 638 convolutional layer, which comprises three convolution layers with $N_f = 32$
 639 channels of kernel sizes 1, 2, and 8. The three convolution layers are concatenated
 640 at the channel dimension. Batch normalization is applied to the output of the
 641 concatenate layers. Finally, rectifier nonlinearity is applied to the output of batch
 642 normalization, and the resulting $[m, \omega, 3N_f]$ matrix is passed to the convolutional
 643 blocks layer.

644 **Convolutional Blocks (Module 2).** The convolutional blocks layer of the
 645 differential-neural distinguisher model is the same as SPECK32/64, except that
 646 the shape of the input is different.

647 **Prediction Head (Output).** The prediction head consists of a GlobalAverage-
 648 pooling layer and an output unit using a *Sigmoid* activation function.

649 **Rationale.** The network architecture for training differential-neural differentia-
 650 tors for SPECK32/64 and SIMON32/64 is essentially the same, except for the
 651 prediction head. Using multiple fully connected layers can lead to an overload of
 652 model parameters and increase the model training time. Therefore, an attempt
 653 is made to use a GlobalAveragePooling layer instead of multiple fully connected
 654 layers.

655 6.2 The Training of Differential-Neural Distinguisher

656 **Training Using the Basic Scheme.** We used two different numbers of training
 657 and test sets to train the neural network. The first situation of experiments
 658 uses N/m and M/m instances as training and test sets. The second situation of
 659 experiments uses N and M instances as the training and test sets. Refer to
 660 the basic training scheme of SPECK32/64 in Sect. 3 for training parameters.
 661 By modifying the network architecture and using the basic training scheme, we
 662 trained the differential-neural distinguisher to recognize the output pairs of 9,
 663 10, and 11-round SIMON32/64 with the input difference (0x0000, 0x0040).

664 **Training Using the Staged Training Method.** A 12-round differential-
 665 neural distinguisher of SIMON32/64 was trained using several pre-training stages.
 666 First, we use our 11-round distinguisher to recognize a 9-round SPECK32/64 with
 667 the input difference (0x0440, 0x0100) (the most likely difference to appear three
 668 rounds after the input difference (0x0000, 0x0040)). The training was done in
 669 10^7 instances for 20 epochs with a learning rate of 10^{-4} . Then we trained the dis-
 670 tinguisher to recognize 12-round SPECK32/64 with the input difference (0x0000,

671 0x0040) by processing 10^7 freshly generated instances for 10 epochs with a learn-
 672 ing rate of 10^{-4} . Finally, the learning rate was dropped to 10^{-5} after processing
 673 another 10^7 new instances each.

674 6.3 Result

675 **Test Accuracy.** We summarize the accuracy of 9, 10, 11, and 12-round differential-
 676 neural distinguisher in Table 5. In addition, we list Acc, TPR, and TNR tested
 677 on newly generated data in Table 6. The 9, 10, and 11-round distinguisher was
 678 trained using the basic training method. Using the staged training method, a
 679 12-round distinguisher was derived from an 11-round distinguisher. We also use
 680 two different numbers of instances to train the differential-neural distinguisher
 681 for SIMON32/64, both for the fair comparison of the experiment and to solve the
 682 problem of overfitting (refer to Appendix C). Compared to gohr’s work [13], the
 683 length of the distinguisher was increased by 1 round, although the accuracy of
 684 the differential-neural distinguisher was not improved.

Table 5. Summary accuracy of the distinguisher on SIMON32/64 using different number of instances

r	$m=1$		[13]*	$m=2$		[13]*	$m=4$	
	[3]	[13]*		N/m	N		N/m	N
9	0.6532	0.661	0.730	0.7251	0.7240	0.811	0.7991	0.8095
10	0.5629	0.567	0.598	0.5917	0.5907	0.637	0.6239	0.6339
11	0.5173	0.520	0.529	0.5193	0.5240	0.543	0.5343	0.5387
12	-	-	-	-	-	-	-	-
r	$m=8$		N	$m=16$		N		
	[13]*	N/m		[13]*	N/m			
9	0.896	0.8774	0.8958	0.963	0.9344	0.9630		
10	0.692	0.6716	0.6900	0.761	0.7230	0.7608		
11	0.563	0.5441	0.5591	0.589	0.5339	0.5878		
12	-	-	0.5152	-	-	0.5225		

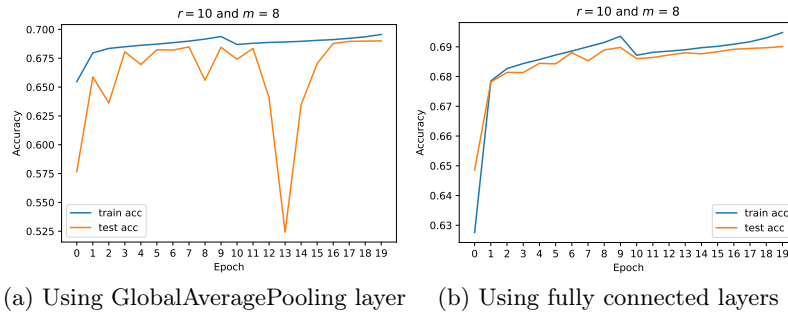
1. *: combining the scores of multiple distinguishers trained by using single-ciphertext pair under independence assumption.
2. The combination method used in [13] is the same as that in [5], which evaluates the distinguisher score of each element in multiple ciphertext pairs, and then takes the median of the results. When the distinguisher is directly trained with multiple ciphertext pairs, the accuracy of the distinguisher will be reduced. For details, see Sect.3.3

685 **Accuracy Fluctuations.** The neural network designed for SPECK32/64 to train
 686 the differential-neural distinguisher uses multiple fully connected layers as pre-
 687 diction heads, resulting in too many model parameters, making training time

Table 6. Acc, TPR, TNR of distinguisher on SIMON32/64 using N instances

m	r	Acc	TPR	TNR	m	r	Acc	TPR	TNR
2	9	0.7234	0.7022	0.7446	4	9	0.8101	0.7821	0.8382
	10	0.5902	0.4779	0.7022		10	0.6347	0.5570	0.7124
	11	0.5155	0.8618	0.1663		11	0.5344	0.7139	0.3550
	12	-	-	-		12	-	-	-
8	9	0.8956	0.8811	0.9101	16	9	0.9630	0.9595	0.9664
	10	0.6908	0.6846	0.6953		10	0.7619	0.7207	0.8030
	11	0.5592	0.5946	0.5239		11	0.5871	0.5338	0.6406
	12	0.5159	0.5324	0.4995		12	0.5218	0.5445	0.4991

688 too long. To address this issue, we use a GlobalAveragePooling layer instead
 689 of the fully connected layer as the prediction head in the neural network of
 690 SIMON32/64. From Fig. 9a and 9b, it can be seen that using the GlobalAver-
 691 agePooling layer will cause relatively large fluctuations in the accuracy, but the
 692 accuracy has almost no effect.

**Fig. 9.** Using different number of instances with different prediction head

693 **Wrong Key Response Profile.** The *wrong key response profile* for our 9, 10,
 694 11, and 12-round differential-neural distinguisher is shown in Fig. 10. As we can
 695 see from the figure when the Hamming Distance between the real key and the
 696 guessed key is smaller, the score of the differential-neural distinguisher is higher,
 697 and vice versa, it is smaller. Judging how far the guessed key deviates from
 698 the real key is easy. This shows that our differential-neural distinguisher can
 699 effectively distinguish between ciphertext and random numbers. In addition, it
 700 can be observed that the score of the distinguisher is higher when the difference
 701 between the guessed key and the real key belongs to $\{8192, 16384, 24576, 32768,$

702 40960, 49152, 57344}, where $r = 10$ and 11, the vertical coordinates of "*" 703 correspond to these positions. This means that when the 13th, 14th, and 15th 704 bits of the subkey are guessed incorrectly, it has little effect on the score of the 705 distinguisher. Therefore, reducing the key guessing space by not guessing these three bits and accelerating the key recovery attack is possible.

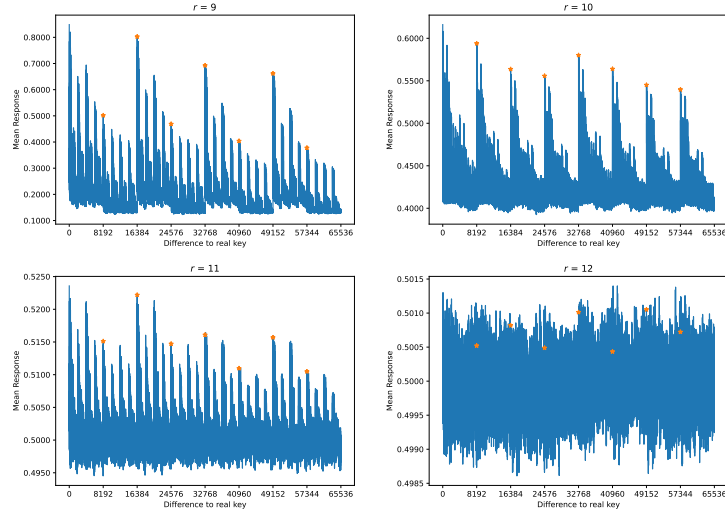


Fig. 10. Wrong key response profile for SIMON32/64 using N instances where $m = 8$

706

707 7 Key Recovery Attack on Round-Reduced SIMON32/64

708 Under a similar procedure to the key recovery attack on SPECK32/64, trained 709 differential-neural distinguishers can be prepended with a classical differential to 710 perform key recovery attacks for SIMON32/64. We improved the 16-round and 711 devised the first 17-round differential-neural-distinguisher-based key recovery at- 712 tacks on SIMON32/64. Note that based on the features found from the *wrong key* 713 *response profile*, we did not guess the 14th and 15th bits of the subkey in the 714 key recovery attack for 16-round SIMON32/64, and 13th, 14th, and 15th of the 715 subkey in the key recovery attack for 17-round SIMON32/64. Sadly, we could not 716 successfully perform the 18-round key recovery attack for SIMON32/64 due to 717 the lack of a sufficient number of generalized neutral bits.

718 7.1 Key Recovery Attack on 16-round SIMON32/64

719 To verify the performance of our 11-round differential-neural distinguisher, the 720 following experiments were carried out in this subsection.

721 **Experiment 3:** The components of the key recovery attack $\mathcal{A}^{\text{SIMON16R}}$ of
722 the 16-round SIMON32/64 are shown below.

- 723 1. 3-round classical differential (0x0440, 0x1000) \rightarrow (0x0000, 0x0040);
724 2. generalized neutral bits of generating multiple-ciphertext pairs: {[2], [3], [4]};
725 generalized neutral bits of combined response of differential-neural distinguisher:
726 {[6], [8], [9], [10], [18], [22], [0, 24], [12, 26]} (refer to Table 11).
727 3. 11-round differential-neural distinguisher $\mathcal{N}\mathcal{D}^{\text{SIMON11r}}$ under difference (0x0000,
728 0x0040) and its wrong key response profiles $\mathcal{N}\mathcal{D}^{\text{SIMON11r}} \cdot \mu$ and $\mathcal{N}\mathcal{D}^{\text{SIMON11r}} \cdot \delta$.
729 4. 10-round differential-neural distinguisher $\mathcal{N}\mathcal{D}^{\text{SIMON10r}}$ under difference (0x0000,
730 0x0040) and its wrong key response profiles $\mathcal{N}\mathcal{D}^{\text{SIMON10r}} \cdot \mu$ and $\mathcal{N}\mathcal{D}^{\text{SIMON10r}} \cdot \delta$.

731 In the beginning, we guess two key bits of k_0 , that is, $k_0[1]$ and $k_0[3]$, because
732 of the 3-round differential, the conditions for correct pairs are $x_1[1] = x'_1[1] = 0$
733 and $x_1[3] = x'_1[3] = 0$. Thus, n_{kg} is 2^2 . However, to make the experimental
734 verification economic, we tested the core of the attack with the two conditions
735 being fulfilled only. The concrete parameters used in our 16-round key recovery
736 attack $\mathcal{A}^{\text{SIMON16R}}$ are listed below.

	$n_{kg} = 2^2$	$m = 8$	$n_b = 2^8$	$n_{cts} = 2^8$
737	$n_{it} = 2^9$	$c_1 = 37, c_2 = 70$	$n_{byit1} = n_{byit2} = 5$	$n_{cand1} = n_{cand2} = 32$

738 The data complexity is $2^2 \times 2^8 \times 2^8 \times 8 \times 2 = 2^{22}$ plaintexts. In total,
739 100 trials are running, and there are 80 successful trials, that is, $sr = 80\%$.
740 The average run time of the experiment is 1115.42s. Thus, the time complexity
741 $T_{\mathcal{N}\mathcal{D}} = n_{kg} \times rt \times 2^{28} \times 2^{2.92} = 2^2 \times 1115.42 \times 2^{28} \times 2^{2.92} = 2^{40.12+2.92}$; $T_{\mathcal{D}\mathcal{D}} =$
742 $n_{kg} \times rt \times \frac{E_s}{R} \times 2^{2.92} = 2^2 \times 1115.42 \times \frac{2^{25.48}}{16} \times 2^{2.92} = 2^{33.60+2.92}$.

743 7.2 Key Recovery Attack on 17-round SIMON32/64

744 Combining a 4-round classical differential with an 11-round differential-neural
745 distinguisher, we examine how far a practical attack can go on 17-round SI-
746 MON32/64 in this subsection.

747 **Experiment 4:** The components of the key recovery attack $\mathcal{A}^{\text{SIMON17R}}$ of
748 the 17-round SIMON32/64 are shown below.

- 749 1. 4-round classical differential (0x1000, 0x4440) \rightarrow (0x0000, 0x0040);
750 2. generalized neutral bits of generate multiple-ciphertext pairs: {[2], [6], [12,
751 26]} (refer to Table 12); generalized neutral bits of combined response of
752 differential-neural distinguisher: {[10, 14, 28]} and five neutral bits conditioned
753 on $x[1, 15], x[15, 13], x[13, 11], x[11, 9], x[9, 7]$ (refer to Table 13).
754 3. 11-round differential-neural distinguisher $\mathcal{N}\mathcal{D}^{\text{SIMON11r}}$ under difference (0x0000,
755 0x0040) and its wrong key response profiles $\mathcal{N}\mathcal{D}^{\text{SIMON11r}} \cdot \mu$ and $\mathcal{N}\mathcal{D}^{\text{SIMON11r}} \cdot \delta$.
756 4. 10-round differential-neural distinguisher $\mathcal{N}\mathcal{D}^{\text{SIMON10r}}$ under difference (0x0000,
757 0x0040) and its wrong key response profiles $\mathcal{N}\mathcal{D}^{\text{SIMON10r}} \cdot \mu$ and $\mathcal{N}\mathcal{D}^{\text{SIMON10r}} \cdot \delta$.

758 In the beginning, we guess two key bits of k_0 , that is, $k_0[3]$ and $k_0[5]$, because
 759 of the 4-round differential, the conditions for correct pairs are $x_1[5] = x'_1[5] = 0$
 760 and $x_1[3] = x'_1[3] = 0$; and six key bits $k_0[1], k_0[15], k_0[13], k_0[11], k_0[9], k_0[7]$
 761 for employing five conditional neutral bits (refer to Table 13). Thus, n_{kg} is 2^8 .
 762 However, to make the experimental verification economic, we tested the core of
 763 the attack with the eight conditions being fulfilled only. The concrete parameters
 764 used in our 17-round key recovery attack $\mathcal{A}^{\text{SIMON17R}}$ are listed below.

$n_{kg} = 2^8$	$m = 8$	$n_b = 2^6$	$n_{cts} = 2^{11}$
$n_{it} = 2^{12}$	$c_1 = 15, c_2 = 65$	$n_{byit1} = n_{byit2} = 5$	$n_{cand1} = n_{cand2} = 32$

766 The data complexity is $2^8 \times 2^6 \times 2^{11} \times 8 \times 2 = 2^{29}$ plaintexts. In total, 100
 767 trials are running, and 9 successful trials, that is $sr = 9\%$. The average running
 768 time of the experiment is 2435.63s. Thus, the time complexity $T_{\mathcal{ND}} = n_{kg} \times rt \times$
 769 $2^{28} \times 2^{2.92} = 2^8 \times 2435.63 \times 2^{28} \times 2^{2.92} = 2^{47.25+2.92}$; $T_{\mathcal{DD}} = n_{kg} \times rt \times \frac{E_s}{R} \times 2^{2.92} =$
 770 $2^8 \times 2435.63 \times \frac{2^{25.48}}{17} \times 2^{2.92} = 2^{40.64+2.92}$.

771 8 Conclusion

772 In this paper, we designed a new network architecture to train differential-neural
 773 distinguisher, which uses multiple-parallel convolution layers to capture the fea-
 774 tures of different dimensions of cryptographic algorithms. As a result, we im-
 775 proved the accuracy and obtained the distinguisher with more rounds. Focusing
 776 on the problem under the same data distribution, we propose a solution using
 777 neutral bits with probability one to generate multiple-plaintext pairs. The com-
 778 bination of multiple improvements reduces the time complexity and increases
 779 the number of rounds of the key recovery attack.

780 References

- 781 1. Abed, F., List, E., Lucks, S., Wenzel, J.: Differential cryptanalysis of round-reduced
 782 simon and speck. In: FSE. Lecture Notes in Computer Science, vol. 8540, pp. 525–
 783 545. Springer (2014)
- 784 2. AlKhzaimi, H., Lauridsen, M.M.: Cryptanalysis of the SIMON family of block
 785 ciphers. IACR Cryptol. ePrint Arch. p. 543 (2013)
- 786 3. Bao, Z., Guo, J., Liu, M., Ma, L., Tu, Y.: Enhancing differential-neural cryptanal-
 787 ysis. In: ASIACRYPT (1). Lecture Notes in Computer Science, vol. 13791, pp.
 788 318–347. Springer (2022)
- 789 4. Beaulieu, R., Shors, D., Smith, J., Treatman-Clark, S., Weeks, B., Wingers, L.: The
 790 SIMON and SPECK families of lightweight block ciphers. IACR Cryptol. ePrint
 791 Arch. p. 404 (2013)
- 792 5. Benamira, A., Gérard, D., Peyrin, T., Tan, Q.Q.: A deeper look at machine
 793 learning-based cryptanalysis. In: EUROCRYPT (1). Lecture Notes in Computer
 794 Science, vol. 12696, pp. 805–835. Springer (2021)
- 795 6. Biham, E., Chen, R.: Near-collisions of SHA-0. In: CRYPTO. Lecture Notes in
 796 Computer Science, vol. 3152, pp. 290–305. Springer (2004)

- 797 7. Biryukov, A., Roy, A., Velichkov, V.: Differential analysis of block ciphers SIMON
798 and SPECK. In: FSE. Lecture Notes in Computer Science, vol. 8540, pp. 546–570.
799 Springer (2014)
- 800 8. Biryukov, A., Cardoso dos Santos, L., Teh, J.S., Udovenko, A., Velichkov, V.: Meet-
801 in-the-filter and dynamic counting with applications to speck. In: International
802 Conference on Applied Cryptography and Network Security. pp. 149–177. Springer
803 (2023)
- 804 9. Chen, Y., Shen, Y., Yu, H., Yuan, S.: A new neural distinguisher considering fea-
805 tures derived from multiple ciphertext pairs (2021)
- 806 10. Dinur, I.: Improved differential cryptanalysis of round-reduced speck. In: Selected
807 Areas in Cryptography. Lecture Notes in Computer Science, vol. 8781, pp. 147–164.
808 Springer (2014)
- 809 11. Feng, Z., Luo, Y., Wang, C., Yang, Q., Liu, Z., Song, L.: Improved differential
810 cryptanalysis on speck using plaintext structures. Cryptology ePrint Archive (2023)
- 811 12. Gohr, A.: Improving attacks on round-reduced speck32/64 using deep learning.
812 In: CRYPTO (2). Lecture Notes in Computer Science, vol. 11693, pp. 150–179.
813 Springer (2019)
- 814 13. Gohr, A., Leander, G., Neumann, P.: An assessment of differential-neural distin-
815 guishers. Cryptology ePrint Archive (2022)
- 816 14. He, K., Zhang, X., Ren, S., Sun, J.: Deep residual learning for image recognition.
817 In: CVPR. pp. 770–778. IEEE Computer Society (2016)
- 818 15. Hu, J., Shen, L., Sun, G.: Squeeze-and-excitation networks. In: CVPR. pp. 7132–
819 7141. Computer Vision Foundation / IEEE Computer Society (2018)
- 820 16. Huang, G., Liu, Z., van der Maaten, L., Weinberger, K.Q.: Densely connected
821 convolutional networks. In: CVPR. pp. 2261–2269. IEEE Computer Society (2017)
- 822 17. Kingma, D.P., Ba, J.: Adam: A method for stochastic optimization. In: ICLR
823 (Poster) (2015)
- 824 18. Song, L., Huang, Z., Yang, Q.: Automatic differential analysis of ARX block ciphers
825 with application to SPECK and LEA. In: ACISP (2). Lecture Notes in Computer
826 Science, vol. 9723, pp. 379–394. Springer (2016)
- 827 19. Szegedy, C., Liu, W., Jia, Y., Sermanet, P., Reed, S.E., Anguelov, D., Erhan, D.,
828 Vanhoucke, V., Rabinovich, A.: Going deeper with convolutions. In: CVPR. pp. 1–
829 9. IEEE Computer Society (2015)
- 830 20. Wang, N., Wang, X., Jia, K., Zhao, J.: Differential attacks on reduced SIMON ver-
831 sions with dynamic key-guessing techniques. *Sci. China Inf. Sci.* **61**(9), 098103:1–
832 098103:3 (2018)

833 A Used Generalized Neutral Bit-sets for Key Recovery 834 Attack

835 A.1 Generalized Neural Bit-sets for SPECK32/64 [3]

836 Neutral bit-sets (NB) Used in [12] for 2-round Classical Differential: The signal
837 from the distinguisher will rather be weak. Gohr boosts it by using $|NB|$ prob-
838 abilistic neutral bits to create from each plaintext pair. A plaintext structure
839 consisting of $2^{|NB|}$ plaintext pairs that are expected to pass the initial 2-round
840 classical differential together. Concretely, neutral bits that are probabilistically
neutral are summarized as follows.

Table 7. (Probabilistic) single-bit neutral bit for 2-round Classical Differential (0x0211, 0x0a04) \rightarrow (0x0040, 0x0000) of SPECK32/64 [12]

NB	Pr.	NB	Pr.	NB	Pr.	NB	Pr.	NB	Pr.	NB	Pr.	NB	Pr.
[20]	1	[21]	1	[22]	1	[14]	0.965	[15]	0.938	[23]	0.812	[7]	0.806
[30]	0.809	[0]	0.763	[8]	0.664	[24]	0.649	[31]	0.644	[1]	0.574		

841

842 Simultaneous-neutral bit-sets (SNBS) used in [3] for 2-round classical differ-
843 ential: for the prepended 2-round differential on top of differential-neural distin-
844 guisher, Bao *et al.* [3] can experimentally obtain 3 complete NB and 2 SNBS using
845 an exhaustive search. Concretely, for the 2-round differential (0x0211, 0x0a04) \rightarrow
846 (0x0040, 0x0000), bit and bit-sets that are (probabilistically) (simultaneous-
)neutral are summarized in Table 8.

Table 8. (Probabilistic) SNBS for 2-round Classical Differential (0x0211, 0x0a04) \rightarrow (0x0040, 0x0000) of SPECK32/64 [3]

NB	Pr.	NB	Pr.	NB	Pr.	NB	Pr.	NB	Pr.	NB	Pr.	NB	Pr.
[20]	1	[21]	1	[22]	1	[9,16]	1	[2,11,25]	1	[14]	0.965	[15]	0.938
[6,29]	0.91	[23]	0.812	[30]	0.809	[7]	0.806	[0]	0.754	[11,27]	0.736	[8]	0.664

847

848 Conditional simultaneous-neutral bit-sets (CSNBS) used in [3] for 3-round
849 classical differential: Bao *et al.* found that there are three sufficient conditions
850 for a pair $(x, y), (x', y')$ to conform to the 3-round differential (0x8020, 0x4101) \rightarrow
851 (0x0040, 0x0000), summarized in Table 9. Concretely, for the 3-round four sub-
852 optimal differential, bit and bit-sets that are (probabilistically) conditional simul-
853 taneous-neutral are summarized in Table 10.

Table 9. Three sufficient conditions conform the 3-round sub-optimal differential [3]

(0x8020, 0x4101)	(0x8060, 0x4101)	(0x8021, 0x4101)	(0x8061, 0x4101)
↓	↓	↓	↓
(0x0040, 0x0000)	(0x0040, 0x0000)	(0x0040, 0x0000)	(0x0040, 0x0000)
$x[7] = 0$	$x[7] = 0$	$x[7] = 0$	$x[7] = 0$
$x[5] \oplus y[14] = 1$	$x[5] \oplus y[14] = 0$	$x[5] \oplus y[14] = 1$	$x[5] \oplus y[14] = 0$
$x[15] \oplus y[8] = 0$	$x[15] \oplus y[8] = 0$	$x[15] \oplus y[8] = 1$	$x[15] \oplus y[8] = 1$

Table 10. (Probabilistic) (simultaneous-)neutral bit-sets for 3-round differential $(0x8020, 0x4101) \rightarrow (0x0040, 0x0000)$, $(0x8060, 0x4101) \rightarrow (0x0040, 0x0000)$, $(0x8021, 0x4101) \rightarrow (0x0040, 0x0000)$, $(0x8061, 0x4101) \rightarrow (0x0040, 0x0000)$ of SPECK32/64 [3]

Bit-set	(8020, 4101)		(8060, 4101)		(8021, 4101)		(8061, 4101)		Condition
	Pre.	Post.	Pre.	Post.	Pre.	Post.	Pre.	Post.	
[22]	0.995	1.000	0.995	1.000	0.996	1.000	0.997	1.000	-
[20]	0.986	1.000	0.997	1.000	0.996	1.000	0.995	1.000	-
[13]	0.986	1.000	0.989	1.000	0.988	1.000	0.992	1.000	-
[12,19]	0.986	1.000	0.995	1.000	0.993	1.000	0.986	1.000	-
[14,21]	0.855	0.860	0.874	0.871	0.881	0.873	0.881	0.876	-
[6,29]	0.901	0.902	0.898	0.893	0.721	0.706	0.721	0.723	-
[30]	0.803	0.818	0.818	0.860	0.442	0.442	0.412	0.407	-
[0,8,31]	0.855	0.859	0.858	0.881	0.000	0.000	0.000	0.000	-
[5,28]	0.495	1.000	0.495	1.000	0.481	1.000	0.469	1.000	$x[12] \oplus y[5] = 1$
[15,24]	0.482	1.000	0.542	1.000	0.498	1.000	0.496	1.000	$y[1] = 0$
[4,27,29]	0.672	0.916	0.648	0.905	0.535	0.736	0.536	0.718	$x[11] \oplus y[4] = 1$
[6,11,12,18]	0.445	0.903	0.456	0.906	0.333	0.701	0.382	0.726	$x[2] \oplus y[11] = 0$

854 Among the two 3-round differentials $(0x8020, 0x4101) \rightarrow (0x0040, 0x0000)$ and
855 $(0x8060, 0x4101) \rightarrow (0x0040, 0x0000)$ are adjoining differentials. The bit 5 of x
856 (the bit 21 of $x \parallel y$) is the SBfADs of both pairs. An SBfADs plays the same role
857 as a deterministic unconditional NB, thus is better to be used than probabilistic
858 and conditional NBs. Specifically, employing SBfADs saves one guessed key bit
859 and reduces both time and data complexity by half compared to employing the
860 CSNBS.

861 A.2 Generalized Neural Bit-sets for SIMON32/64 [3]

For an input pair $((x, y), (x', y'))$ to conform to the 3-round differential $(0x0440, 0x1000) \rightarrow (0x0000, 0x0040)$, one has conditions that

$$\begin{cases} x[1] = x'[1] = 0 \\ x[3] = x'[3] = 0 \end{cases}$$

Table 11. NB and SNBS for 3-round Classical Differential $(0x0440, 0x1000) \rightarrow (0x0000, 0x0040)$ of SIMON32/64 [3]

[2]	[3]	[4]	[6]	[8]	[9]
[10]	[18]	[22]	[0,24]	[12,26]	

862

For an input pair $((x, y), (x', y'))$ to conform to the 4-round differential $(0x1000, 0x4440) \rightarrow (0x0000, 0x0040)$, one has conditions that

$$\begin{cases} x[5] = x'[5] = 0 \\ x[3] = x'[3] = 0 \end{cases}$$

Table 12. NB and SNBS for 4-round Classical Differential $(0x1000, 0x4440) \rightarrow (0x0040, 0x0000)$ of SIMON32/64 [3]

[2]	[6]	[12,26]	[10,14,28]
-----	-----	---------	------------

Table 13. CSNBS for 4-round Classical Differential $(0x1000, 0x4440) \rightarrow (0x0040, 0x0000)$ of SIMON32/64 [3]

Bit-set	C.	Bit-set	C.	Bit-set	C.	Bit-set	C.	Bit-set	C.
$x[1, 15]$		$x[15, 13]$		$x[13, 11]$		$x[11, 9]$		$x[9, 7]$	
[24,10]	00	[22,8]	00	[20]	00	[18,4]	00	[16,8]	00
[24,10,9]	10	[22,8,7]	10	[20,5]	10	[18,4,3]	10	[16,8,1]	10
[24,10,0]	01	[22,8,14]	01	[20,12]	01	[18,4,10]	01	[16]	01
[24,10,9,0]	11	[22,8,7,14]	11	[20,12,5]	11	[18,4,3,10]	11	[16,1]	11

C.: Condition on $x[i, j]$, e.g., $x[i, j] = 10$ means $x[i] = 1$ and $x[j] = 0$.

863 B Procedure of $(1 + s + r + 1)$ -round key recovery attack

864 The attack procedure is as follows.

- 865 1. Initialize variables $Gbest_{key} \leftarrow (\text{None}, \text{None})$, $Gbest_{score} \leftarrow -\infty$.
- 866 2. For each of the n_{kg} guessed key bits, on which the conditions depend,
 - 867 (a) Generate n_{cts} random data with difference ΔP , and satisfying the con-
868 ditions being conforming pairs (refer to Appendix A).

- 869 (b) Using n_{cts} random data and $\log_2 m$ neutral bit with probability one to
870 generate n_{cts} data pairs. Every data pairs have m data.
- 871 (c) From the n_{cts} random data pairs, generate n_{cts} structures using the n_b
872 generalized neutral bit.
- 873 (d) Decrypt one round using zero as the subkey for all data in the structures
874 and obtain the n_{cts} plaintext structure.
- 875 (e) Query for the ciphertexts under $(1 + s + r + 1)$ -round SPECK or SIMON
876 of the $n_{cts} \times n_b \times 2$ plaintext structures, thus obtaining n_{cts} ciphertext
877 structures, denoted by $\{\mathcal{C}_1, \dots, \mathcal{C}_{n_{cts}}\}$.
- 878 (f) Initialize an array ω_{\max} and an array n_{visit} to record the highest distin-
879 guisher score obtained so far and the number of visits have received in
880 the last subkey search for the ciphertext structures.
- 881 (g) Initialize variables $best_{score} \leftarrow -\infty$, $best_{key} \leftarrow (\text{None}, \text{None})$, $best_{pos} \leftarrow$
882 None to record the best score, the corresponding best recommended val-
883 ues for the two subkeys obtained among all ciphertext structures and the
884 index of these ciphertext structures.
- 885 (h) For j from 1 to n_{it} :
- 886 i. Compute the priority of each of the ciphertext structures as follows:
887 $s_i = \omega_{\max i} + \alpha \cdot \sqrt{\log_2 j / n_{\text{visit}i}}$, for $i \in \{1, \dots, n_{cts}\}$, and $\alpha = \sqrt{n_{cts}}$;
888 The formula of priority is designed according to a general method in
889 reinforcement learning to achieve automatic exploitation versus explo-
890 ration trade-off based on Upper Confidence Bounds. It is motivated to
891 focus the key search on the most promising ciphertext structures [12].
- 892 ii. Pick the ciphertext structure with the highest priority score for fur-
893 ther processing in this j -th iteration, denote it by \mathcal{C} , and its index by
894 idx , $n_{\text{visit}idx} \leftarrow n_{\text{visit}idx} + 1$.
- 895 iii. Run the BAYESIANKEYSEARCH Algorithm [12] with \mathcal{C} , the r -round
896 differential-neural distinguisher $\mathcal{N}\mathcal{D}^r$ and its wrong key response pro-
897 file $\mathcal{N}\mathcal{D}^r \cdot \mu$ and $\mathcal{N}\mathcal{D}^r \cdot \sigma$, n_{cand1} , and $n_{\text{byit}1}$ as input parameters;
898 obtain the output, that is, a list L_1 of $n_{\text{byit}1} \times n_{cand1}$ candidate
899 values for the last subkey and their scores, i.e., $L_1 = \{(g_{1i}, v_{1i}) : i \in$
900 $\{1, \dots, n_{\text{byit}1} \times n_{cand1}\}\}$.
- 901 iv. Find the maximum $v_{1\max}$ among v_{1i} in L_1 , if $v_{1\max} > \omega_{\max idx}$,
902 $\omega_{\max idx} \leftarrow v_{1\max}$.
- 903 v. For each of recommended last subkey $g_{1i} \in L_1$, if the score $v_{1i} > c_1$,
- 904 A. Decrypt the ciphertext in \mathcal{C} using the g_{1i} by one round and obtain
905 the ciphertext structures \mathcal{C}' of $(1 + s + r)$ -round SPECK or SIMON.
- 906 B. Run BAYESIANKEYSEARCH Algorithm with \mathcal{C}' , the differential-
907 neural distinguisher $\mathcal{N}\mathcal{D}^{r-1}$ and its wrong key response profile
908 $\mathcal{N}\mathcal{D}^{r-1} \cdot \mu$ and $\mathcal{N}\mathcal{D}^{r-1} \cdot \sigma$, n_{cand2} , and $n_{\text{byit}2}$ as input parameters;
909 obtain the output, that is a list L_2 of $n_{\text{byit}2} \times n_{cand2}$ candidate
910 values for the last subkey and their scores, i.e., $L_2 = \{(g_{2i}, v_{2i}) :$
911 $i \in \{1, \dots, n_{\text{byit}2} \times n_{cand2}\}\}$.
- 912 C. Find the maximum v_{2i} and the corresponding g_{2i} in L_2 , and de-
913 note them by $v_{2\max}$ and $g_{2\max}$.

914 D. If $v_{2\max} > best_score$, update $best_score \leftarrow v_{2\max}$, $best_key \leftarrow (g_{1i}, g_{2\max})$,
 915 $best_pos \leftarrow idx$.
 916 vi. If $best_score > c_2$, go to Step 2i.
 917 (i) Make a final improvement using VERIFIERSEARCH [12] on the value of
 918 $best_key$ by examining whether the scores of a set of keys obtained by
 919 changing at most 2 bits on top of the incrementally updated $best_key$
 920 could be improved recursively until no improvement is obtained, up-
 921 date $best_score$ to the best score in the final improvement; If $best_score >$
 922 $Gbest_score$, update $Gbest_score \leftarrow best_score$, $Gbest_key \leftarrow best_key$.
 923 3. Return $Gbest_key, Gbest_score$.

924 **C Overfitting in training differential-neural distinguisher**
 925 **with N/m and N instances**

926 From Fig. 11, 13, 15, 17, 19, we can see that the difference between training
 927 accuracy and test accuracy is relatively large. Therefore, using N/m and M/m
 928 instances as training and test sets to train a neural network will suffer from
 929 overfitting, especially when the number of rounds r and m is large. However, the
 930 difference between training accuracy and test accuracy is very small and almost
 931 equal in Fig. 12, 14, 16, 18, 20. Therefore, using N and M instances as training
 932 and test sets to train the differential-neural distinguisher can avoid overfitting,
 933 speed up the model convergence, and improve the model accuracy to a certain
 934 extent.

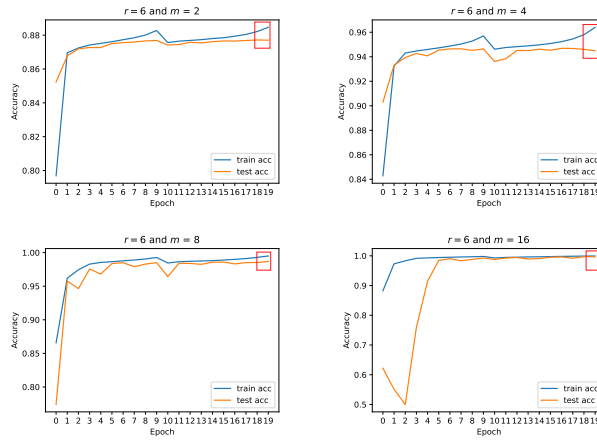


Fig. 11. Using N/m instances for 6-round SPECK32/64

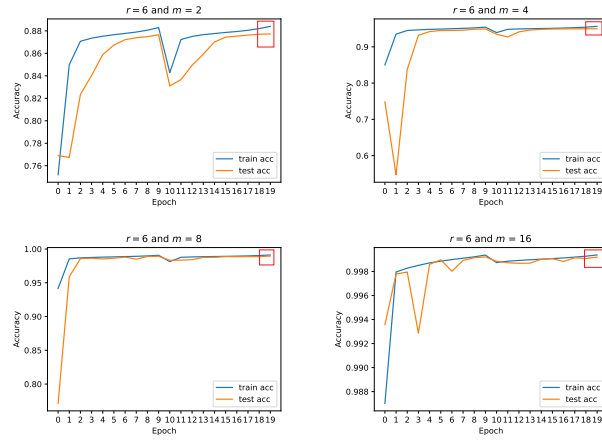


Fig. 12. Using N instances for 6-round SPECK32/64

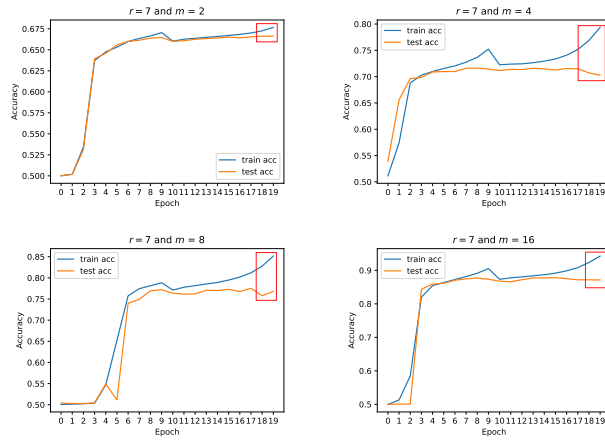


Fig. 13. Using N/m instances for 7-round SPECK32/64

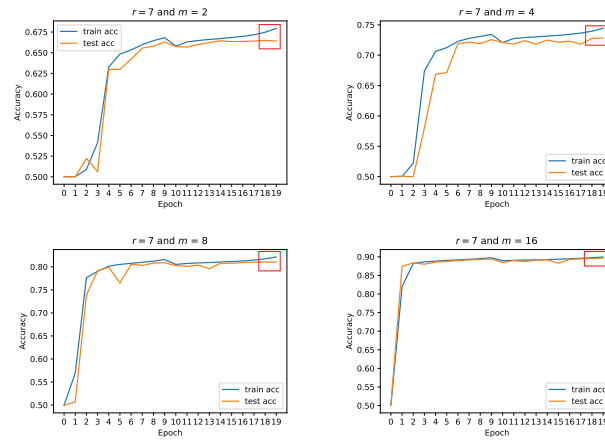


Fig. 14. Using N instances for 7-round SPECK32/64

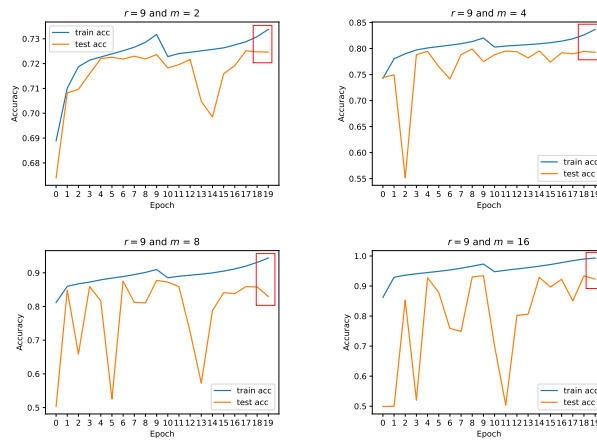


Fig. 15. Using N/m instances for 9-round SIMON32/64

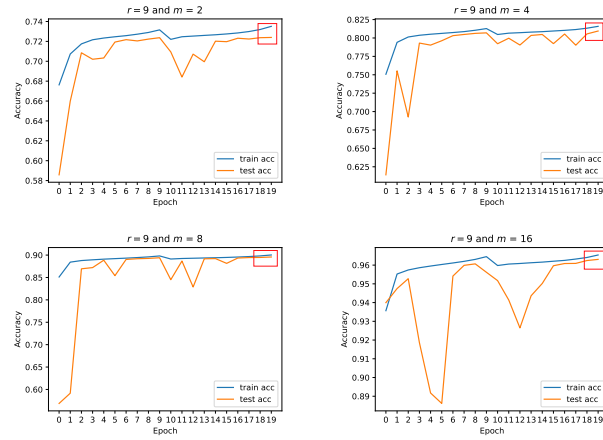


Fig. 16. Using N instances for 9-round SIMON32/64

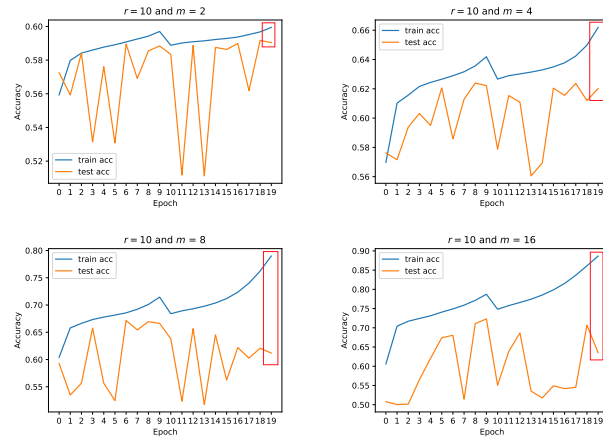


Fig. 17. Using N/m instances for 10-round SIMON32/64

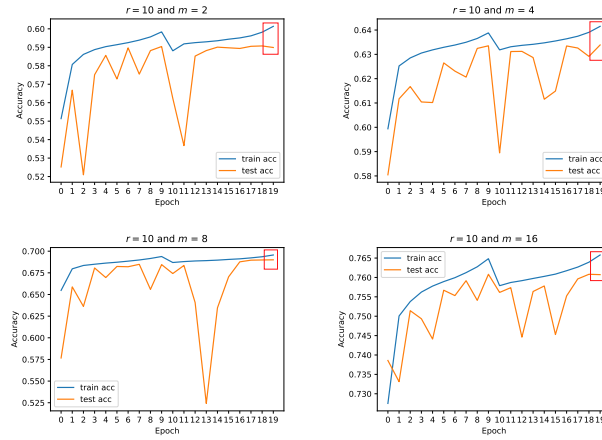


Fig. 18. Using N instances for 10-round SIMON32/64

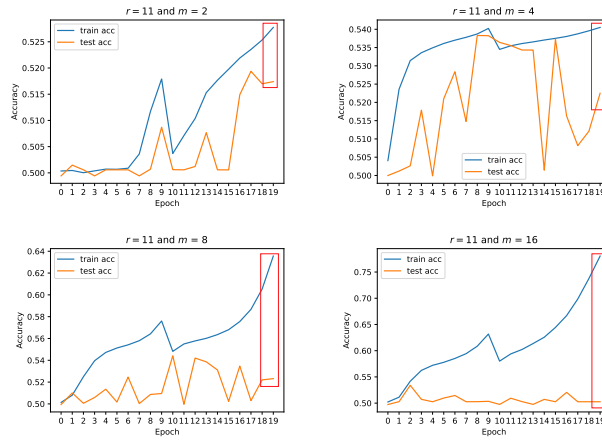


Fig. 19. Using N/m instances for 11-round SIMON32/64

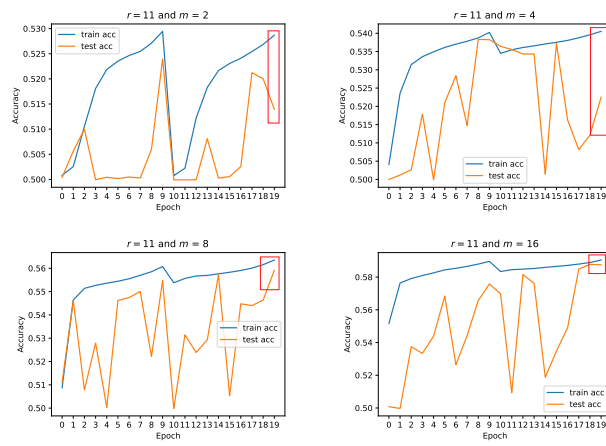


Fig. 20. Using N instances for 11-round SIMON32/64